Journal of Nanomaterials & Molecular Nanotechnology

Review Article

In vivo General Trends, Filtration and Toxicity of Nanoparticles

Grant A Hartung[1] and G Ali Mansoori[1]*

Abstract

The medical field is a vastly expanding one and with the discovery of nanoparticles (carbon nanotubes, diamondoids, fullerenes, gold and silver nanoparticles, quantum dots, etc.), there lies a vast field of unsolved medical diagnoses to be reassessed. Upon reassessment of the current medical problems, it is important to know what happens to a particle once it is free in the body. This review examines the different destinations of nanomaterials after they enter the body, their toxicity and their filtration. Assessing the destination of nanoparticles is done in order to find out whether they are removed by macrophages. It is concluded the strongest trends of the nanoparticles itself is of shape and surface chemistry. Toxicity of nanoparticles is found to be mostly dose-dependent. The nanoparticle filtration goal is to have the body naturally filter out the nanoparticles without a response from the immune system.

Introduction

In the field of biology, there exists a series of subcategories which are independently studied and incorporated into daily life. Of these subcategories, there exists a category named nano-biotechnology. This is a category which is a cross section between fields of biology, chemistry, engineering and physics. These fields all come together to produce many different types of products that hold extremely valuable and unique characteristics [1-3] that can solve many of the most challenging biological problems of today's world [4].

Quantum dots are a type of nanostructure comprised of a two-part core, an inner core and an outer core. These nanostructures are frequently synthesized with metal molecules for the core and are spherical in shape. They can then be polymerized with different lengths and types of polymers on their surface to both make them more biocompatible and more tissue selective. When the quantum dots become tissue selective and are targeted to cancerous tissues, they are capable of being excited via photon absorption and can elicit fluorescent resonant energy transfer (FRET) *in vivo* that causes lipid peroxidation and cell death.

Fullerenes are a type of carbon-based molecule. Graphene, fullerenes, and carbon nanotubes (including both single and multi-walled) are comprised of carbon atoms formed in pentagons and

hexagons. Fullerenes that are comprised of bonds that form 20 hexagonal ring formations and 12 pentagonal ring formations with 60 atoms of carbon are called C_{60} and create a ball-shaped configuration and can even be as large as C_{240} (240 carbon atoms) [5]. Each carbon atom is bonded to 2 other carbon atoms with single bonds. The bonds that are shared between 2 adjacent hexagonal rings observe van der Waals interactions that have stronger bond strength and are chemically written like a second bond (Figure 1 (Left)). The double bond signifies the stronger bond strength which results in the carbon atoms being physically closer together as can be seen by the bond lengths written in figure 1 (Left). It is possible to break the van der Waals "bonds" in fullerenes in order to attach other molecules or scavenge free radicals in the body [6,7]. Through this, it is possible to functionalize the fullerenes by doing things such as making them polar (and thus water-soluble) or functionalizing their size and chemistry to make them tissue-specific.

Another important characteristic to the C_{60} fullerenes is that its diameter is 0.71 nm from nucleus-to-nucleus (entire molecule diameter, not the distance between adjacent atoms). Having it so small allows it to be highly mobile in the body and be able to pass through many different membranes in the body in order to accomplish its function (including the blood-brain barrier) [6,7]. Given that the average red blood cell is on the order of 10 μm, this allows the fullerenes to be able to even jump the membrane into individual cells, something that can be extremely useful in the new age of medicine.

Carbon nanotubes (CNTs) are a sub-type of fullerene. This is a distinction based on the chemistry of the molecule. CNTs also share the hexagonal/pentagonal formation of carbon atoms with alternating double/single bonds. These molecules are of great interest in many different parts of the medical field because they have an extremely high electrical conductivity and tensile strength for their size and weight. It is due to this that CNT toxicology is reported to be of interest [8]. They are also hollow so there has been much attention paid to flow through them [9,10] and the production of them [11].

Single-walled carbon nanotubes have a wall that is only one carbon atom thick and they have, when compared to multi-walled nanotubes, higher electrical conductivity and strength per weight yet multi-walled carbon nanotubes are stronger in a one-on-one test. Multi-walled carbon nanotubes are multiple single-walled nanotubes placed concentrically around the same axis.

Diamondoids generously get their name relation to diamonds due to their immensely rigid structure and density of the bonds between the carbon atoms. Diamondoid architecture is also known to be cage-like, have a self-assembly nature and be capable of functionalization [12-14]. Adamantane is a diamondoid of much interest in the medical field as it is the lowest diamondoid (least number of carbon atoms per molecule) and research of its atomic forces have revealed its uniquely high electrical conductivity [15,16].

A derivative of adamantane named memantine has been used in the pharmaceutical industry for many years (Figure 1 Right) [6,7] and is also capable of self assembly [14]. It is known to have many unique

***Corresponding author:** G Ali Mansoori, Department of Bioengineering, University of Illinois, 851 S. Morgan St. (MC 063), Chicago, IL, 60607, USA, Tel: +1-312-996-5592; E-mail: mansoori@uic.edu
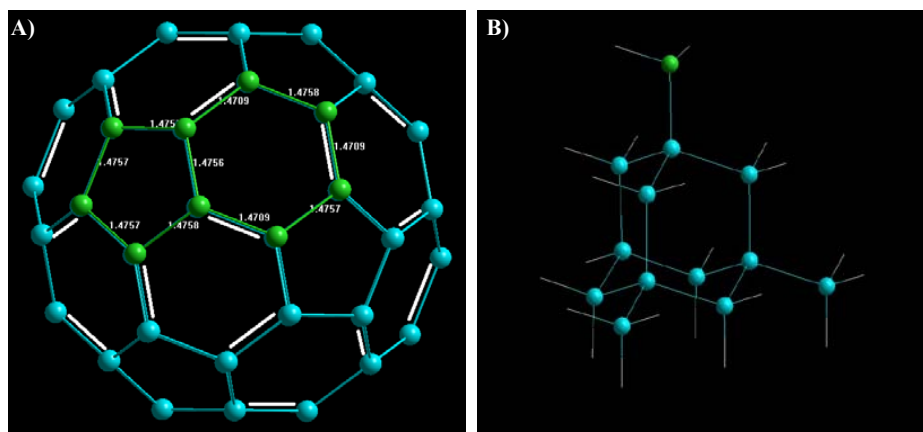
Figure 1: (A) A single C_{60} fullerene created using HyperChem. The bond lengths shown are in angstroms, the shorter bonds are written as a double bond (white) to signify their increased strength and decreased proximity (1.4758 angstroms vs 1.4709 angstroms). (B) A memantine diamondoid. Blue atoms are carbon, white sticks are hydrogen atoms, and the green atom is nitrogen.

characteristics in response to neuroreceptors in the brain. It is also polar due to the NH_2 group and extra carbon atoms. This increases the use and interest in this particle's possibilities.

Gold has much research interest in the field of cancer treatment due to its ability to be thermally excited [6,7,17-22]. Both silver and gold have been used in Alzheimer's research previously [7]. Gold and silver nanoparticles are both considered inert and naturally hydrophobic so their passing through the body is limited. They have much potential due to their small size yet the biodistribution is still not entirely clear for either particle. This is largely attributed to attack from the immune system to such inert and non-polar particles when they have low functionalization. It is due to this that there has been much research in trying to derive a more organic version of silver nanoparticles to lower their innate toxicity [6,23,24].

Liposomes are a unique type of nanostructure that has many capabilities. It is composed of a lipid bilayer and is capable of surface functionalization and encapsulating other nanoparticles for drug delivery. It is known that they can be broken down by lysosomal enzymes within blood cells where an encapsulated drug can then take effect [25]. Due to their hydrophilic nature and surface functionalization capabilities, liposomes are highly investigated for use with tissue-specific drug delivery of toxic particles [26-38].

The first reaction of the immune system is the same no matter what type or of what nature the invader is. This is a response called the "innate" immune system response. This response is designed to kill effectively everything. It is a system of total eradication spawned by neutrophils which are designed to kill invading particles, bacteria, and even healthy cells (which could be in the process of being mutated or infected as they are being killed). Neutrophils are not the only part, but they are the main contributor to factors such as reactive oxygen species proliferation which leads to the degradation of cellular membranes through a process known as lipid peroxidation. This process leads to cell death and has been frequently consistent with *in vivo* findings in nanoparticle research.

The second type of immune response is called "adaptive" immune response. This is the response of such items as T and B cells which are designed to kill foreign viruses outside of cells and kill cells infected

and mutated by viruses/bacteria in a more specialized and unique way for each invader. Another type of adaptive immuno response, one of importance in this review, is that of the reticuloendothelial system (RES) comprised of phagocytic cells (mainly monocytes and macrophages). Phagocytes such as macrophages are cells that encapsulate foreign bodies and attempt to degrade them over time through such processes as peroxidation.
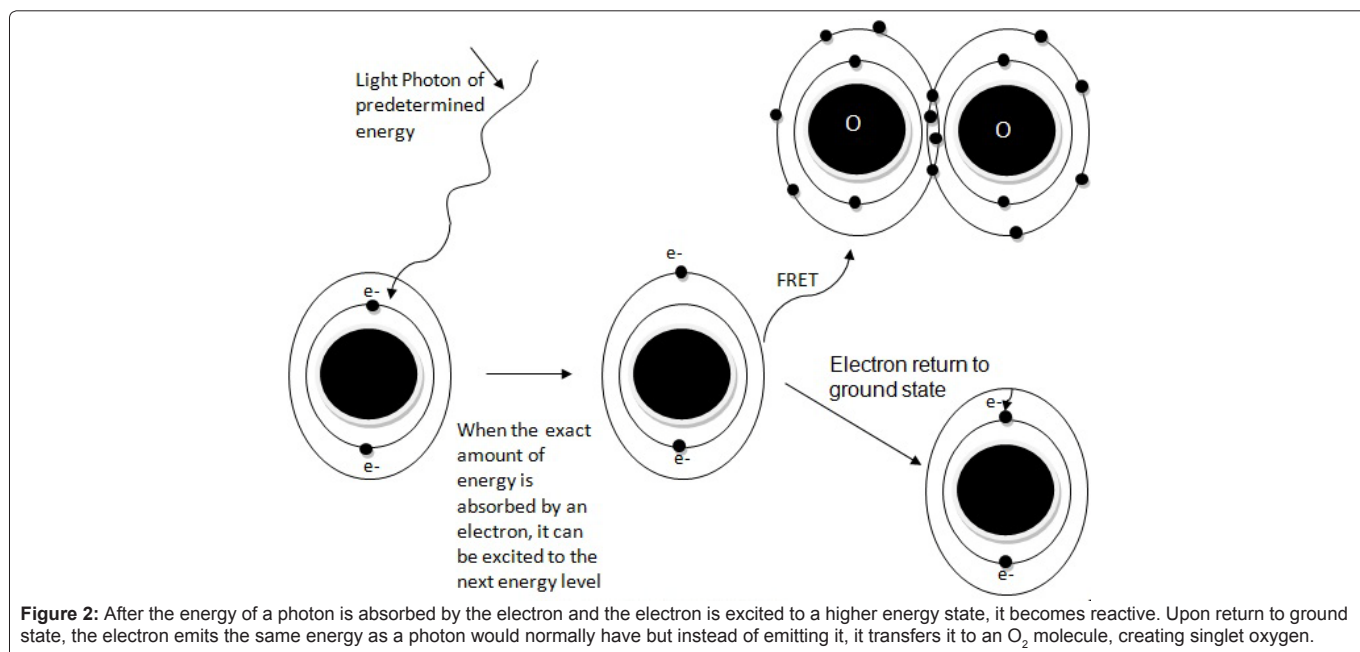
The body also has liquid excretory system that filters things out of the body and digestive system to filter out what enters the blood stream if particle is ingested. These are also of high importance in this review as many particles can be filtered out naturally similar to how proteins and food are filtered. This is, of course, the easiest system which eliminates nanoparticles from the body and thus is the most favored. If a nanoparticle is to be engineered, the filtration goal is to have the body naturally filter out the nanoparticles without an inflammatory response from the immune system.

The recently highlighted topics of interest by the US Environmental Protection Agency (EPA) include the toxicology of manufactured nanoparticles [39]. One of the most important factors of toxicology is biofiltration, cytotoxicity post administration. Much attention has been paid to the affects of the nanoparticles to the body but very little attention has been paid to how the body affects the nanoparticles or how the body reacts to the nanoparticles after they are in the body. The question to be asked is: do the particles get degraded by the immune system, encapsulated by the immune system, filtered out by natural filtration methods designed for waste material, or just get trapped in the body and accumulate until organ failure or death? This is a comprehensive review of the biofiltration of nanoparticles to assess the processes that the nanoparticles undergo once in the body.

Advances in Nanotechnology

Quantum dots

It has been previously reported that fluorescent resonance energy transfer (FRET), shown in figure 2, can be an efficient and extremely useful process in quantum dot (QD) research in fighting cancerous tissues through a process called lipid peroxidation [40-42]. Regular

Figure 2: After the energy of a photon is absorbed by the electron and the electron is excited to a higher energy state, it becomes reactive. Upon return to ground state, the electron emits the same energy as a photon would normally have but instead of emitting it, it transfers it to an O_2 molecule, creating singlet oxygen.

energy fluorescence can also be used to visualize tissues [43-46]. FRET is a method that can be both useful and completely toxic depending on how it is utilized.

Most QDs are created via non-biocompatible organic metals and are hydrophobic [47-52]. To decrease the hydrophobicity of the QDs, in an effort to keep them from agglomerating, they are often coated. This increases their size and hinders their ability to be eliminated from the body (when over a certain size, the particles are seen as invasive as opposed to naturally occurring proteins) [53]. The effects of agglomeration, due to not coating the particles, creates entrapment into tissues like the liver [54]. The polymerization of hydrophilic ligands stops this agglomeration and maintains hydrophilicity which keeps entrapment to a minimum [54] so the increase in particle size due to polymerization still seems to be the better choice.

Previous research was able to confirm the short term effects of the QD samples being different than the long-term effects (Figure 3) [47,53,54]. In the short term, the QDs accumulated in the liver, and in the long term, in the kidneys (Figure 3) [47,53]. It was also noticed that the size of the QD particles made a difference. The smaller sized particles were more readily absorbed by the kidneys and the larger ones by the liver (Figures 3-5) [47,54]. The spleen was targeted by a very select size range (5.3-5.6 nm with polyethylene glycol (PEG) coating and 2.9 nm uncoated) (Figure 5). It was also seen that there were no toxic effect after 80 days after a single intravenous (IV) injection evident in the rats, thus helping to prove that synthetic aqueous QDs can be non-toxic [47].

It was found that the largest distinction between the different metabolic processes were not based entirely on chemical interactions but rather also on size (Figure 5) [47,50,51,53,54]. The more agglomerated the particles in the body, the more likely they are to be absorbed by the liver and passed as urea [53]. This is unless they agglomerate too large in which there is no longer any metabolic function to remove them from the body and they agglomerate in tissues or get absorbed by the RES [47,54]. It was noticed that the

free QDs were filtered by glomerular capillaries [55] (the capillaries at the beginning of the kidney which function to filter the blood) and excreted through urine whereas most of the QDs attached to proteins and agglomerated to larger forms were filtered through the liver [55].

Choi et al. [53] indicated that traditional, uncoated QDs are between 10 and 100 nm in diameter and have proven difficult to be cleared from the body [54]. They go further to say the QDs are frequently engulfed by the immune system [47,54]. Using transmission electron microscopy (TEM), it was verified that the core diameter (Indium-Arsenic Zinc-Sulfide core (InAs(ZnS)) was averaged at 3.2 nm [54]. PEG chains have been proven in prior research to increase solubility and delay the immune response to such particles. In this study, the lengths of PEG chains varied from 0 to 22 repeating units.

An increase in the PEG chain length resulted in an increase in the blood retention time, renal excretion, and delayed extravasations from affected tissues [55]. The "shorter" chain length QDs (diameter less than or equal to 5.5 nm) were partially absorbed and cleared by the kidneys as liquid waste where they were stable however a large number of these particles were attacked by the RES system in the liver, consistent with previous research [53,54]. The "larger" chain length (diameter over 5.5 nm) QDs were absorbed and cleared by the liver into bile [54]. A noteworthy exception was the PEG8 (6.5 nm) group were found in the pancreas [54].

It was noted that if the diameter becomes too small (less than 5.5 nm), the body's immune system attacks the molecule and attempts to degrade it using the RES as is noted in table 1. In this process, the macrophages engulf the QD and begin to eat away, or depolymerize the PEG coating, exposing the toxic core. The toxic core of the QD is then able to cause detriment to all cells it comes into contact with and no successful response by the body to facilitate its motion out of the body is present [47].

The semiconductor QDs which are made up of Cadmium-Sulfide (CdS), Cadmium-Selenium (CdSe), or Cadmium-Tellurium (CdTe)
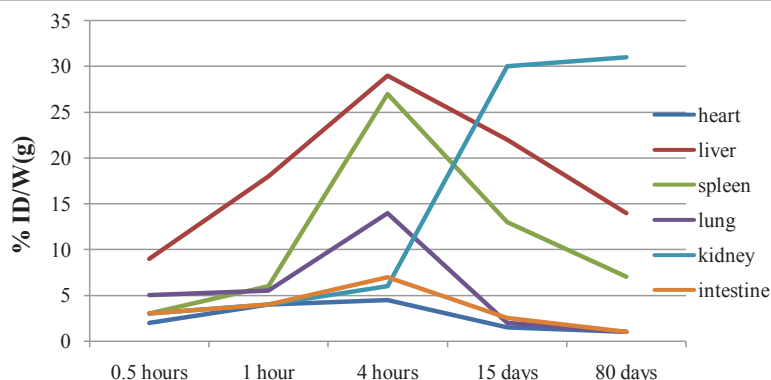
Figure 3: Biodistribution at different times of 2.9 nm CdTe aqueous QDs. Vertical axis is % of injected dose/weight of tissue (in grams). Data derived from previous research [47].
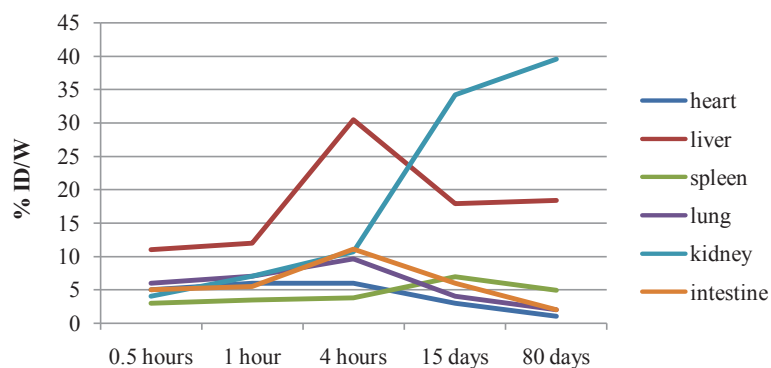

Figure 4: Biodistribution at different times of 4.5 nm CdTe aqueous QDs. Vertical axis is % of injected dose/weight of tissue (in grams). Data derived from previous research [47].
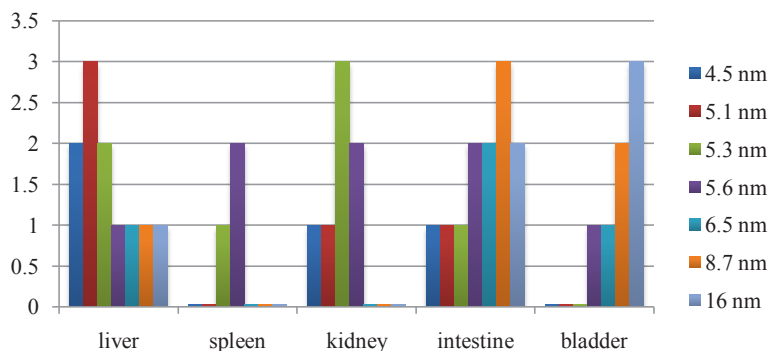

Figure 5: Biodistribution at 4 hours post-injection of InAs core and ZnS shell QDs polymerized with different lengths of Poly-ethylene Glycol (PEG) chains. Vertical axis based on simplified data categorized by integers 0, 1, 2, and 3 corresponding to density of QDs in organ from least dense to most dense respectively [54].

have been known to emit morphological changes in cells, increase lipid peroxidation, decrease cell viability, and depress metabolic activity upon excitation or exposure of the core [47,53,54]. This is not unlike the reaction of the immune system to invasive bodies. Many of the physiological changes in the cells related to the exposure to these QDs take place in a relatively short time span (within just a few hours of the excitation, consistent with neutrophillic reactions to invasive particles) [47,53,54]. This gives credit to the belief that

surface functionalization and chemistry is a very important part of the biodistribution and cytotoxicity of nanoparticles.

Fullerenes

A study by Baker et al. [56] that compared 3 sets of rats (control, nano-fullerenes (55 nm), and larger nano-fullerenes (930 nm referred to as the "microparticle group")) that were exposed to an aerosol version of natural C_{60} fullerenes. In order to accurately create airborne

Table 1: The general trends of the emerging nanoparticles. The situations which cause reactions from the above listed as "unreactive unless specific conditions are met" are detailed earlier in this review.

	Non-filtering Immune Response	Useful Range	Preferred Shape	Surface Chemistry
PEG Inorganic QD	<5 nm [48]	4-16 nm [56]	Sphere	Polymerized
Organic QD (CdSe/ZnS)**	<5.5 nm [55]	5.5-8.8 nm [55]	Sphere	Protein coated
Gold	<2nm & >= 20nm [136-138]	4-18 nm* [136,137]	Sphere	Inert metal
Silver	All [147,150,152]	8-18 nm ***[152]	Sphere	Inert metal
Memantine	N/A****	1 nm [133]	Polar Non-Sphere	Polar and unreactive
PMC-16	N/A*****	1.8-2 nm [65]	Polar Sphere	Polar and unreactive unless specific conditions are present
C3C$_{60}$	N/A*****	2-8 nm [70,108]	Polar Sphere	Polar and unreactive unless specific conditions are present
NDs	N/A****	2-8 nm [119]	Polar Non-Sphere	Polar and unreactive
SWNT	All [77,84-87]	None yet	Cylinder	Non-Polar and unreactive unless specific conditions are present
MWNT	All [65,66]	None yet	Cylinder	Non-Polar and unreactive unless specific conditions are present
Liposomes	<20 or >200 nm [3,175,176]	20-200 nm³	Sphere	Lipid bilayer
*=more or less depending on zeta potentials [123,125]			**=DHLA coated	
***=most useful range yet with best excretory percentages				
****=natural anti-immunotoxic effects and small size disallows use to elicit toxic response				
*****=applications are of unique particle, size does not vary enough for immune system elicitation				

fullerenes that could be inhaled in a measurable fashion, a process was done to procure an aerosol version of the fullerenes [57] and upon x-ray spectroscopy and high-pressure liquid chromatography (HPLC), it was determined that the aerosol version of the fullerenes matched the solid state in every way.

It was proven in this study that the exposure over 10 days to aerosol fullerenes did not lead to extensive toxicity in the rats [56]. The lung assessments revealed that the particles at different times in the lung decreased as a function of time implying the temporary nature of the adsorption onto the lung tissue [58]. It was also noted that for the nanoparticle group, the adsorption onto the lung tissue was 47% higher than that of the microparticle group. The deposition fraction, percent of total sample that was fixated onto the lung tissue alone, was 14.1% for nanoparticle and 9.3% for microparticle tissues (taken at 10 days) [56].

It was also noted that none of the particles in any group of rats showed traces of fullerenes in the red blood cell samples. It was also noted that the dead cell count rose in the order of control <nanoparticle group <microparticle group (Figure 6). The extensive uptake into the liver is consistent with RES entrapment of hydrophobic fullerenes. The heart and testes both noticed a mild lowering of tissue weight attributed to degradation due to a side effect of adsorption of the particles onto the tissue (Figure 6) possibly from the immune system attacking the particles adsorbed onto the tissue. These findings are consistent with previous research that natural C$_{60}$ particles agglomerate due to their hydrophobic surface chemistry [58,59]. After they agglomerate, the particles get attacked by the body's immune system [54,60-62].

A study by Boushehri et al. [63] explores the use of a C$_{60}$ fullerene derivative as targeted drug delivery. They utilized an ionized isotope of magnesium which could be delivered to doxorubicin-induced damaged heart muscle. This type of damaged heart muscle simulates hypoxia-induced tissue damage (heart attack). The particular fullerene chosen was the iron containing porphyrin monoadduct of the classical C$_{60}$ molecule known as Porphyllerene-MC16 (PMC16).

It was noted that the fullerene acted as a "smart particle" and released the Mg^{2+} in response to increasing acidity of its medium, a phenomenon experienced by hypoxia-related tissue damage [64]. During this experiment there was reported a "total lack" of absorbance of the particles into such "trapping" tissues as kidneys, liver, lungs, and skeletal muscles [63].

A study by Yuan et al. [40] takes a closer look into a different use of fullerenes; radical scavenging and why different derivatives of C$_{60}$ fullerenes are able to differ in their scavenging efficacies. This study introduced superoxide and hydroxyl radicals (naturally occurring as a byproduct of the neutrophilic response of the immune system). The superoxide and hydroxyl radicals were administered to the cell cultures to simulate *in vivo* lipid peroxidation [65-67].

The study had then measured the control of the peroxidation when fullerene derivatives were added. The amount of lipid peroxidation was measured through membrane leakage of staining dies that were administered into the cells prior to the experiment. It is speculated that the mechanism behind the radical scavenging affects of C$_{60}$ derivatives are that the van der Waals interactions between carbon atoms on fullerene cages (of which there are 30 for C$_{60}$ and 27 for C$_3$ and D$_3$ derivatives) can be broken and the radical absorbed by the fullerene [40,58,68]. Polar C$_{60}$ molecules (such as C$_3$ and D$_3$) possess strong antioxidant effects yet do not agglomerate in such a manner as natural fullerenes (due to their being hydrophilic) [40]. The toxicity elicitation concentration of natural C$_{60}$ and C$_3$C$_{60}$ *in vitro* was seen as 20 parts per billion (ppb) and 10,000 ppb respectively [69,70]. In contrast, the in vitro comparison between the radical scavenging affects of C$_3$C$_{60}$ and D$_3$C$_{60}$ can be seen in figure 7a [60].
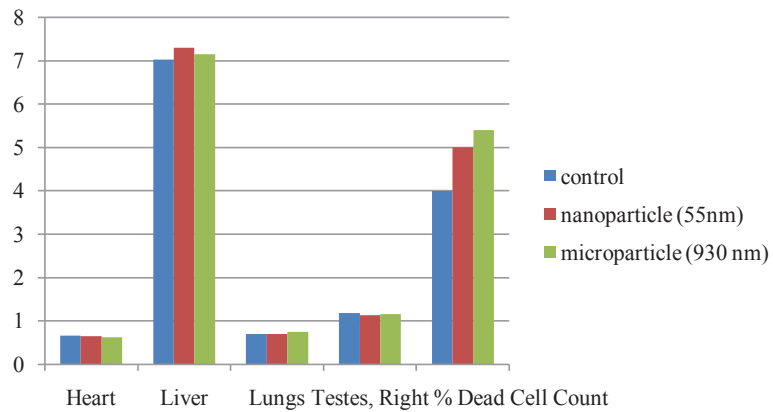
Figure 6: Organ weight in grams post aerosol exposure for 3 hours per day over 10 days. Vertical axis is the final percent dead cell count due to natural C_{60} [56].
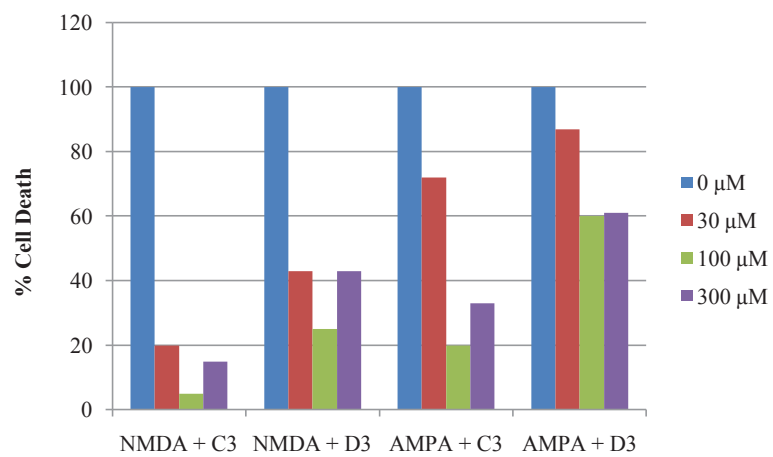

Figure 7a: Cell viability after exposure to cytotoxic media at varying concentrations. Data derived from previous research [60].
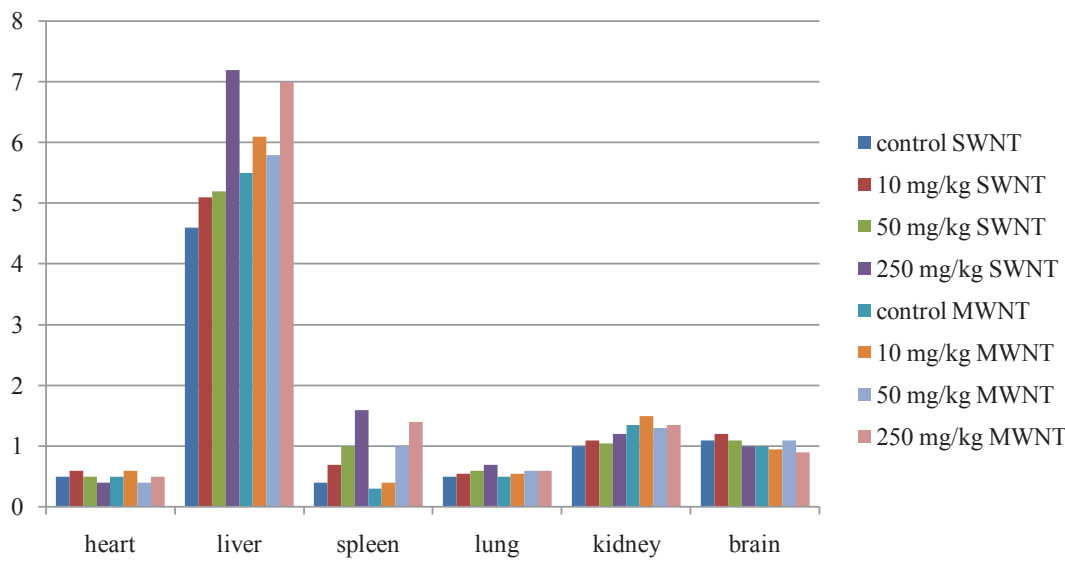

Figure 7b: Vertical axis is the tissue weight as a percentage of body weight in mice. Mice were treated with multi and single-walled carbon nanotubes for 28 days post-injection. Data derived from previous research [80].

A study by Quick et al. [68] attempted to prove the de-oxidant power of the C_3 derivative of C_{60}. This was to be done by reducing oxidative stress that can be recorded by a longer lifespan. An increase in longevity of life was attributed to the reduction in oxidative stress extending to the brain based on previous research linking oxidative stress to natural aging processes [69]. This study is novel in that, aside from calorie restriction processes [71], it is the first successful approach to lengthening the lifespan of mammals, proving the anti-oxidant affects of the C_3 C_{60} molecule [68] and does so by proving its ability to jump the blood brain barrier safely and still be naturally excreted from the body without immune response.

Carbon nanotubes

A study by Mazatenta et al. [72] found that long term neurotoxicity of neuron-carbon nanotube interfaces *in vitro* can be rejected, which is consistent with previous research [73]. This is due to a prevalence of detected spontaneous patterned activity which is present in both the cultured neuronal circuits and the excited neurons through the SWNTs. This indicates that the SWNTs do not inhibit the population firing, which is supported by the finding that the sodium ion (Na^+) current is still fast; an early indication of neuronal differentiation leading to neuronal growth promotion [74].

An experiment by Fiorito et al. [75] was conducted to assess the abilities of fullerenes and SWNTs to elicit an *in-vitro* inflammatory response in murine and human macrophage cells. It also compared to the effects of carbon based nanomaterials to that of graphite. This was done through evaluating the release of nitric oxide (NO, a neurotransmitter for immunoresponse) by the macrophages when excited by fullerenes, SWNTs and graphite particles [76,77].

The uptake of particles into the monocyte-derived macrophages (MDM) cells as a function of time seemed to plateau at 24 hrs for fullerenes as opposed to 48 hrs for SWNTs and even later for graphite. It was established that the percentage of cells exhibiting apoptosis or necrosis were very low (4% and 2%) for SWNTs and fullerenes, respectively, at 48 hours as opposed to 25% with graphite [75]. Not only were the levels of cellular death significantly higher for graphite than experienced in SWNTs but the pattern of toxicity

was very different for graphite as well (it was significantly more toxic) which is consistent with previous research [75,78,79]. The elicitation of macrophage cells was still significant enough to prove the hydrophobic surface chemistry of the nanoparticles can elicit a toxic response *in vitro*.

A more detailed study by Liang et al. [80] injected rats with phosphorylcholine-grafted multi-walled carbon nanotubes (MWCNTs) 10-30 nm diameter and 5-15 micron length. By the end of the investigation, it was noticed that no toxic effects were noticed in the rats that would result in immediate death [80]. A previous study had shown that over a 4 month period, mice had shown no evidence of toxicity that would hinder overall survival [81]. In this study, however, it had seemed that a high level of adsorption of the CNTs onto the liver, spleen, and lungs was present which is consistent with previous research (Figure 7b) [82-85]. This can be attributed to uptake by the RES in the liver and the spleen due to the hydrophobic surface chemistry of the nanotubes.

Recent studies have also explored the study of carbon nanotubes on the plasma membrane of macrophages and observed damage to the membrane which triggered inflammation of the phagocytotic cells [86-89]. Other studies also proposed that epitheloid granuloma can be generally formed if the SWNTs are inserted intratracheally (Figure 8) [90,91]. This is a research topic of much interest because the creation of the CNTs makes them naturally airborne [8,11]. Previous research revealed multiple wall lesions on mice subjects that were dose-dependent which was not seen in the study by Liang et al. [80]. This was attributed to differentiations in the administration techniques and the surface modification of the samples in this study [90].

In a study by Belyanskaya et al. [61] CNTs were first purified and then dispersed in two different agglomeration amounts, a highly agglomerated sample (SWNT-a at 100 nm) and a more thoroughly dispersed sample (SWNT-b at 20 nm). The lowest concentration that revealed a significant change in cellular DNA was 200 μg/ml polyoxyethylene sorbitan monooleate (PS80) [61].

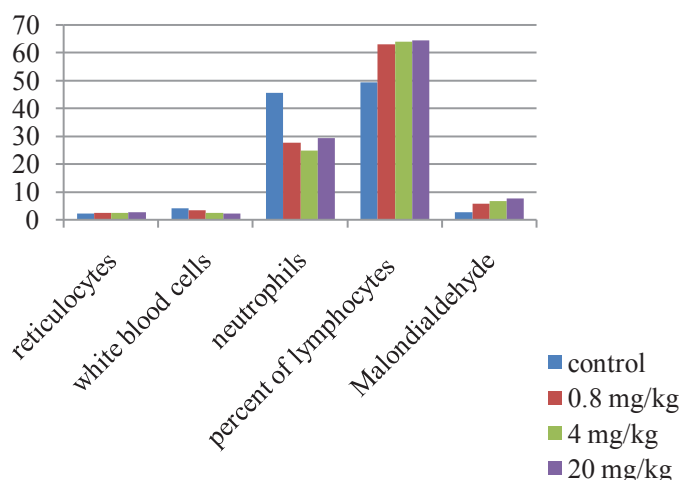The central nervous system (CNS)-derived nervous samples had a

Figure 8: Dose dependent toxicity of 40-100 nm NDs at 4 hours post-intratracheal injection. The vertical axis is as follows: reticulocytes, white blood cells, and percent of lymphocytes are in ×10³/μL, neutrophils are in percent of total cell count, and malondialdehyde is in μmol/L. Data derived from previous research [91].

dose-dependent deterioration of DNA when the highest concentration of SWNTs (30 µg/ml) was administered causing a reduction in DNA of 18% for SWNT-b and 35% for SWNT-a exposed groups [61]. The same phenomenon was also seen for the peripheral nervous system (PNS)-derived samples, with the same maximum concentrations of SWNTs eliciting a reduction in 33% and 58% respectively [61].

An assessment was made as to whether or not the effects were seen via the detriment to the glial cells or if they affected the nerves as a whole. An enriched glial culture had shown a similar pattern to that of the previous experiment, leading to the belief that the glial cells are the main contributor to the decrease in DNA viability over time [61]. At the end of a series of tests it was seen that only the SWNT-b group affected this protein concentration (decreased).

CNTs have a propensity, due to their small size and shape, to get trapped in the lipid bilayer of blood cells and agglomerate in the cytoplasm which leads to rapid cell death [92,93]. It is due to this that the degradation of CNTs has been studied to find a way to remove the CNTs from the blood stream more efficiently. Previous research has proven that free radicals and ROS can react with CNTs and break them down [61]. Myeloperoxidase (MPO) is a natural mediator produced by neutrophils as a part of the body's reaction to infection/invasion by foreign bodies along with ROS [62]. It was also noted that in the presence of blood plasma, even with high concentrations of hemoglobin (another molecule with oxidizing capabilities) and H_2O_2, there was no appreciable degradation of the CNTs [62].

MPO, on top of oxidizing capabilities in degradation of CNTs, creates free halide ions [62]. There was also found an appreciable increase in peroxidase-induced degradation to CNTs during exposure to MPO with the addition of chloride ions. This phenomenon supported the previous belief that hypochlorite (ClO^-) is a considerable contributor to the degradation of CNTs due to its being the product of mixing chloride ions with MPO [93-95]. A two-fold increase in degradation was observed in samples treated with bromide ions over those left untreated [61].

The previous research has shown that a derivative of SWNTs polymerized by PEG both increases the solubility of the SWNTs and decreases the activation of macrophages in response to the SWNTs *in vivo* [96-99]. In the study by Belyanskaya et al. [61], the introduction of PEG to the SWNTs had no effect on the peroxidase-induced degradation of the nanotubes. The degradation of the SWNTs was noted to be maximized by either an MPO/Cl⁻/H_2O_2 mixture or LPO/Br⁻/H_2O_2 mixture [61]. *In vivo,* CNTs absorb plasma proteins but at an order of magnitude slower than the reaction of free radicals with the proteins themselves. Nevertheless, experimentation found no conclusive evidence of substantial CNT degradation *in vivo* [61].

Previous research has also proven that the manufacturing of CNTs creates airborne CNTs in large quantities [98]. A paper by Davboren et al. [99] tests the effects of SWNTs on A549 human lung cells. An appreciable detriment was observed to the cells at all concentrations but in particular a 42% and 51% inhibition were reported in 400 and 800 µg/ml concentrations respectively [85]. This was measured through injecting fluorescent dye into the cells at the beginning and measuring the fluorescence of the entire sample before and after administration. It was seen that when exposed to quartz, the detriment to cells by the SWNTs increased as a function of concentration for 200 and 400 µg/ml concentrations but a decrease in

toxicity at 800 µg/ml [98].

It was noted that one of the challenges to studying the cytotoxicity of SWNTs is their propensity to bundle. In the experiment it was seen (through scanning electron microscopy) even after several washes that bundles of SWNTs were still adhered to the cell surface. It was noticed that quartz exposure to the human lung cells produced the same cytotoxic results as the SWNTs at similar concentrations, supported by previous research [92]. The use of quartz as a comparison for cytotoxicity has been previously reported as a valid practice [90,91,100].

There were morphological changes found through transmission-electron microscopy. Previous research reported morphological changes in the cells due to absorption of the CNTs into cells [101,102]. This was not consistent with this study which was attributed to a lower concentration being administered in this study [99]. It has been recorded that the increase in concentration of SWNTs leads to an increase in lamellar bodies as a reaction from the tissue to the invasive particles [99].

Although many studies such as that by Haval et al. [8] have attempted to attribute the toxicity of CNTs to their impurities, such as iron, commonly found in the samples. It has been noted, however, that cell proliferation decreases as a function of time even in samples exposed to purified nanotubes when compared to control groups [90,103,104].

Nanodiamonds

A study by Zhu et al. [105] had utilized nanodiamonds (NDs) with an average size of 2-8 nm. They are very strong per unit volume yet at low pH they are known to dissociate the carboxyl groups [106] and thus create a significant change in the surface potential. This is not a problem, though, in realistic conditions (pH: ~7.2). *In vitro* studies have proven NDs to be non-toxic and NDs have been seen as the least toxic of all the nanocarbon materials [99]. This study had proven that the cytotoxicity of NDs was extremely relative to which serum proteins the culture was based in [99].

When exposed to lungs, Wang et al. [107] found no trace of the toxic effects of lipid peroxidation on lung cells and concluded low pulmonary toxicity post-intratracheal installation. Upon assessing the destination of the NDs it was concluded that the macrophages were the most effective removal tool for NDs [107]. This could be attributed to the higher concentrations in the ladder study (0.8-20 mg/kg [90] compared to 0.1-1 mg/kg [107]). The lung toxicity of NDs, when compared to other carbon materials, though, is still the lowest [90,91,108].

Further research indicates that NDs are not fatal nor hinder growth of any organ weight dynamics [109]. The reproductive nature and health of all samples was also entirely unaffected for at least the 3 generations tested by Schrand et al. [109]. Other experiments have lead to the observance that there were no inflammatory symptoms or immunotoxicity present after 3 months and 10 days respectively [90,107]. Toxicity was, however, observed in a dose-dependent manner when examined in response to the lung, liver, kidneys and blood stream (Figure 9) [110].

Further studies had shown the general biodistribution (when attached to fluorescing particles) of ND movement arrested in the spleen (consistent with biodistribution based on size) and bones.
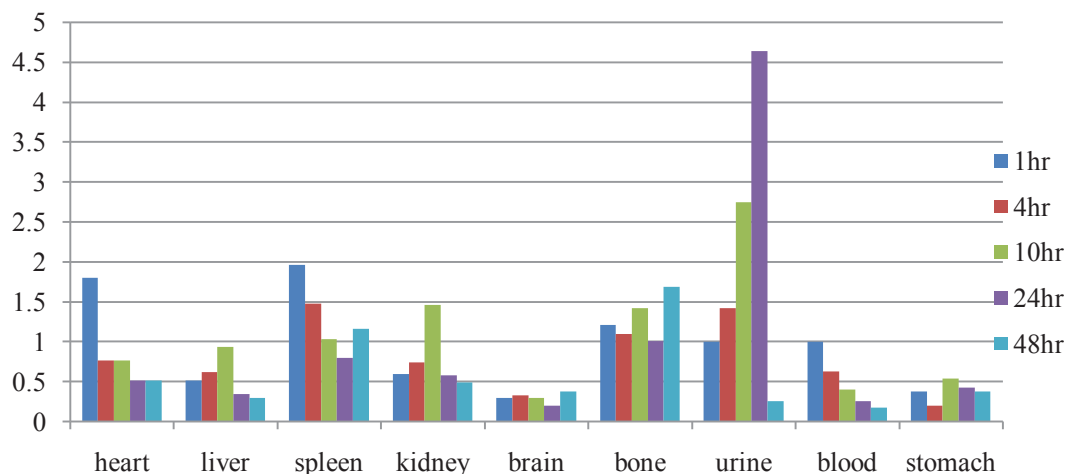
Figure 9: Time-related distribution of 40-100 nm NDs. Vertical axis is organ uptake (organ radioactivity/(total radioactivity*organ weight(g))). Data derived from previous research [110].

The excretory systems are responsible for the majority of the removal from the bloodstream and only minimal traces were found in the bones and heart (Figure 9) [110]. Further examination had shown an accumulation in the lung, liver (60% at 0.5 hrs which kept constant over 28 days), and spleen [111]. Rojas et al. [112] rendered the similar results as above but verified the primary excretory faculty being the urinary tract. It was noticed that when larger particle sizes were filtered out before administration, the lung and spleen uptake were severely inhibited [111].

In a study by Chow et al. [113] 500 microgram doses of NDs (2-8 nm) failed to increase levels of sera interleukin-6 (IL-6). IL-6 is an inflammatory marker of the immune system [113]. Using ND surface complexes the blood circulation halftime was increased by a factor of 10. A significant myelosuppression decrease was also observed through the NDX (nanodiamond complex) treatment (200 microgram of Doxorubicin (Dox) equivalent) compared to Dox treatment of the same concentration [113].

When labeled with XenoFluor 750 and Alexa Fluor 488, it was seen that clearance from the body was achieved in 3-10 days (120 μg) and 1-10 days (40 μg). Clearance was seen as organ-dependent [113]. The clearances were 4 days and 10 days for lung and liver, respectively, and 7 days for the spleen and kidney. It was noted that due to the covalent bonds between the dyes and the NDs that all fluorescing particles were NDs and not free dye [113].

The dye alone (when not attached to the NDs) is cleared from the spleen and lungs in half the time it takes to clear the liver and kidneys (liver and kidneys require 48 hours for full clearance) [113]. This is due to the filtering affects of the excretory and reticuloendothelial systems, so clearance of the spleen and lungs is a tissue-specific clearance whereas clearance from the kidneys and liver reflect total blood circulation clearance [113].

NDs naturally have average cluster sizes of 50 nm and nanodiamond complexes (NDXs) are on the order of ~80 nm [114]. Polydispersion indices ranged from 0.1-0.2 at 25 degrees C (they have a narrow size distribution) [115,116]. Depending on the pH and purification procedure, zeta potentials of nanodiamonds (NDs) have been seen to be around -10 mV [106]. The zeta potential of the

NDs was around 17.7 mV and ND-NH$_2$ was around 48 mV. After being dyed, the zeta potentials change to around -38.8 +/-0.4 mV (ZenoFluor 750) and 27.1 +/- 2 mV (Alexa Fluor 488) [115]. It was noted that the NDX had a higher zeta potential than unmodified NDs at a neutral pH allowing for higher dispersity [101].

Adamantane

A study by Yong and Mansoori [15] provided evidence that the size of adamantane particles and derivatives are on the order of ~1 nm. Adamantane is naturally hydrophobic and has been previously shown to be poorly metabolized in human subjects [117]. Polymerization of PEG, in rats, changes the agglomerationand biodistribution profile [118] from the lung to the liver [119]. Memantine is a polar adamantane derivative that is quite stable and unreactive. Amantadine and memantine are used for Parkinson's disease [120-122] and Alzheimer's disease [123]. Memantine is known to have effects similar to the NMDA channel blocker known as MK-801 [117,124,125].

The use of radiobinding is growing in popularity for adamantane [119,124]. A popular tracer derivative of adamantane is ^{18}F-memantine. A study by Samnick et al. [124] had shown relatively fast clearance; less than 1% of injected dose per gram of organ remained after 240 minutes with only one organ exception: the bladder (Figure 10).

Two tissues were only determined to have radiotracing effects after 60 minutes, the bladder/urine and the feces samples (Figure 10). The feces samples were negligible and the urine increased significantly after the first review of the distribution which was, itself, very high (13.13% of injected dose). The liver had a peak concentration at 30 minutes and the brain experienced a peak at 30 minutes and nearly exactly the same concentration at 30 minutes and 60 minutes. All other organs significantly decreased in concentration after the immediate measurement at 5 minutes to a very low percentage as described above (Figure 10) [124].

The relatively high uptake into the brain indicates a successful ability to jump the blood-brain barrier and with an ability to filter out from the brain (Figure 10) [124]. The uptake in the brain was appreciably higher in the hippocampus and the cerebral cortices of
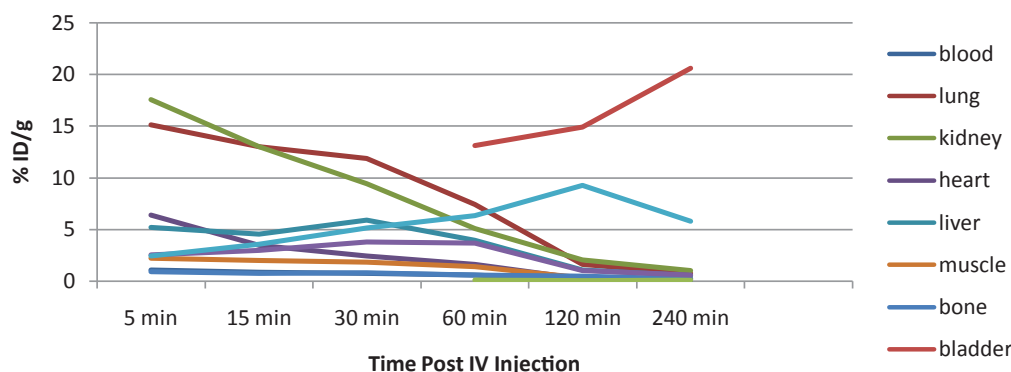
Figure 10: Distribution of ^{18}F-labeled memantine following a single intravenous injection. Vertical axis is percent of injected dose/gram of organ. Data derived from previous research [124].

the rat brains (approx. 75% of brain concentration) which coincide with regions noted for having the highest densities of N-methyl-D-aspartate (NMDA) receptors (which memantine is known to be an NMDA antagonist) [124].

In a study by Ametamey et al. [125] there was an immediate uptake of memantine into the blood in the brain which is quickly removed. The amount of memantine in all other tested parts of the brain, after an almost immediate jump in concentration, increased over the entire experiment. The white matter occasionally had uptake consistent with a 2-tissue compartmental model even though it does not contain NMDA receptors [126]. In contrast, the striatum and frontal cortex better followed a 1-tissue compartmental model even though they were rich in NMDA receptors [126]. The general observation was that it was homogenously distributed amongst gray matter and less dispersion was present amongst white matter. This shows a clear ability for memantine to jump the blood-brain barrier safely without toxic effects.

Gold nanoparticles

Gold (Au) is relatively insoluble as a substance so it is rare in natural biological systems. Previous research using human K562 leukemia cells [127] utilized gold nanoparticles (AuNPs) of sizes 4, 12, and 18 nm in diameter and were shown to not pose any toxicity, consistent with previous research [128]. This is in contrast with AuNPs of diameter 1-2 nm were seen as highly toxic in both healthy and cancerous cells [127-130]. Another study that utilized 20 nm AuNPs had shown that oxidative stress was present in embryonic lung fibroblasts which led to inhibited cell proliferation (likely due to immune reactions) [131].

This and other studies have shown that AuNPs accumulate primarily in the liver and spleen regardless of size, shape or dose (Figure 11) [132-134]. This in consistent with previous beliefs that non-polar NPs are subject to uptake by the RES in the liver. The Kupffer cells (a specialized type of macrophage) in the liver have been seen to bind to 40 nm Au particles and clusters remained in the liver even after 6 months [135].

The findings of the lung tissues in relation to the control were consistent with the belief that the lungs act as a temporary reservoir for the AuNPs [133,134]. In previous research 77% of IV administered AuNPs at 1.9 nmdiameter were passed within 5 hours of injection [136].

A study by Jong et al. [132] had checked the effect of size using 10, 50, 100, and 250 nm AuNPs. Of all the groups of nanoparticles, the 10 nm group was the only group to have a presence of gold in the brain [132]. The 10 and 100 nm groups were the highest blood, liver and spleen retention whereas the highest adsorption onto the lung tissue was the 50 nm group which had adsorbed 8-fold more than the 10 nm group. All groups except for the 10 nm group were dispersed entirely among the liver, spleen and blood (Figure 11) [132].

Particle sizes in a study by Sonavane et al. [131] were 15, 50, 100, and 200 nm with zeta potentials -42.9, -40.9, -40.8, and -35.9 mV respectively. It was noted that previous research has effectively narrowed possible zeta potentials for stable suspension being greater than 30 mV or less than -30 mV [135]. Each group (with the exception of the 200 nm group) was shown to contain particles that had a hydrodynamic diameter (hdd) less than 25 nm which have been seen to jump the blood-brain barrier without too much difficulty [132].

It was noted that size, hydrophobicity, and surface biocompatibility are what govern the biodistribution patterns of nanoparticles under 100 nm [132]. It was noticed that the blood concentration of Au was filtered out entirely by 72 hours which was supported by previous research [136] with PEG-polymerized Au particles with hdd of 89+/-3.1 nm. This shows evidence of altered surface chemistry changing the biofiltration patterning of AuNPs.

Silver nanoparticles

Silver ions are known to be toxic to all kinds of bacteria and plant life [137-139]. The natural reaction of the body to silver nanoparticles is known to elicit ROS and create mitochondrial oxidative stress [140]. The elicitation of ROS is from the immune system thus allowing the immune system to react quickly to the silver and, when applied to open wounds, also to the invasive viruses. This is a viable explanation for the antimicrobial affects of the silver nanoparticle (AgNP) ions [137,139-141]. In a study by Kim et al. [140] 60 nm silver nanoparticles (AgNPs) are used in a repeated oral administration over 28 days and the accumulation was noticed in the liver, kidneys and stomach in a dose-dependent manner.

In a different study using subcutaneous injections of 50-100 nm AgNPs it was noticed that not only were the kidneys and liver affected with agglomerations of the NPs but the spleen, lung tissue, and endothelial cells of the blood-brain barrier were also affected [142].
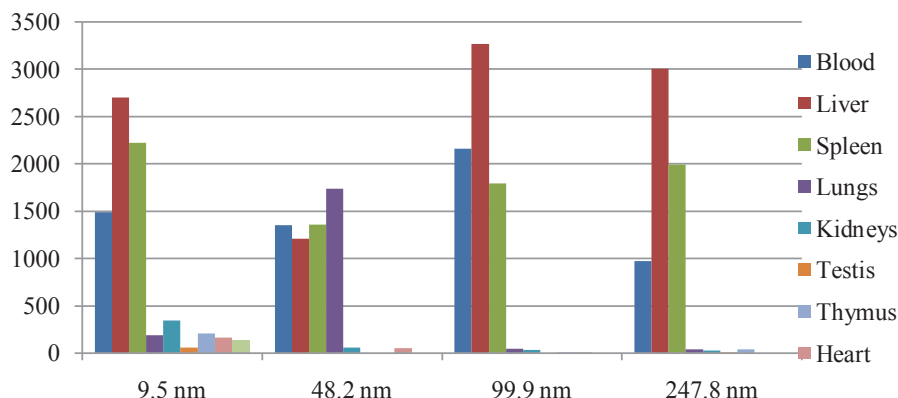
Figure 11: Concentration of gold in organs. The vertical axis is nanograms of gold particles/gram of organ tissue. Measurements were taken 24 hours post-injection to the tail vein in rats. Data derived from previous research [132].

In a third experiment by Garza-Ocañas et al. [143,144], BSA-coated AgNPs with a diameter of 2 nm agglomerated in the liver, kidneys, and the heart tissues but the agglomeration was attributed to the BSA coating reacting with the tissues.

In a study by Loeschner et al. [142] the diameters were 14 nm (90% of particle volume) and 50 nm (11% by volume and 0.1% by count) of orally administered AgNPs. The zeta potential was previously reported to be around -2 mV at pH of 5.9 [145]. Previous research claimed a required zeta potential of ± 30 mV for stable suspension [135] and the uptake into the liver was relatively high. When comparing the distribution *in vivo* of two different Ag nanoparticles (AgNPs and silver acetate (AgAc)) the distribution was highly similar between them [142]. The distribution, in ascending order (AgNP as a percent of AgAc is noted), was in the liver, kidney (40-50%), stomach (40-50%), and small intestine tissues [142]. AgNPs had a lower concentration than the AgAc group in the muscle (10-20%), lung (10-20%), brain (40-50%), kidney (40-50%), and blood plasma (40-50%) tissues [142].

The primary form of excretion of the silver nanoparticles was in solid waste [145-152] and the liquid waste disposal of the nanoparticles was seemingly negligible (<0.1%) [145]. The excretion in feces was 63 ± 23% of the daily dose and 49 ± 21% of daily dose for AgNPs and AgAc respectively [145]. Previous research into intravenous implementation of silver NPs had shown that the concentration ratio of bile-to-plasma concentration of silver NPs was 16-20 factors higher in bile [148].

Previous studies have shown that agglomeration can be seen in tissues *in vivo* [142-148] and that an inflammatory immune response can be elicited by the AgNPs both in vivo and in vitro [149-150]. The well-documented anti-microbial affects that have been seen [30,151,152] could very well have relevance to this. The elicitation of ROS by the silver nanoparticles is the response by the neutrophils to invasive particles which not only could be attacking the AgNPs but also attacking all surrounding tissues, including any bacteria or infected cells.

Liposomes

Liposomes are a unique nanoparticle as they are not only in the general size constraints noticed in other nanoparticles reviewed in this manuscript, albeit it is the largest of them (<200 nm),but they are also capable of encapsulating other nanoparticles that would normally be toxic to the body to release upon particular conditions [26-38]. Particles such as doxorubicin which is used for liver, breast, and ovarian cancer and even AIDS-related Kaposi's Sarcoma can be toxic to the rest of the body yet can be encapsulated by liposomes and be used with tissue specificity [26-38,153,154]. The functionalization of the liposome surface by such things as polymers and proteins allow for specifically engineered extravasation, organ uptake, and avoidance of the RES [30-32,154]. This is due to the entrapped molecule following the pharmacokinetics of the liposome coating instead of the raw molecule [155,156].

An experiment by Gabizon et al. [156] tested the biodistribution of different surface functionalizations of liposomes. The different combinations of tested liposomes were phosphatildylglycerol (PG)-phosphatidylcholine (PC)-cholesterol (Ch), PG-distearoylphosphatidylcholine (DSPC)-Ch, hydrogenated phosphatidylinositol (HPI)-DSPC-Ch, dipalmitoylo-phosphatidylglycerol (DPPM)-DSPC-Ch, and monosialoganglioside (GM)-DSPC-Ch. The different biodistribution studies can be seen in figure 12.

The use of cholesterol in all trials was due to its previously reported ability to help evade the RES [33]. The unique findings of this study had shown a correlation between high liver-to-blood ratios and high liver-to-tumor ratios [156]. It had, however shown, as consistent with previous research, that optimal delivery diameter regardless of coating is ≈100 nm for tumor models [30,156-159]. It was noted, though that even in this range small changes can make a significant difference in the distribution as can be seen in figure 13 [156].

PEG-polymerized liposomes are of much interest in cancer research as they have been previously proven capable of extravasation into tumors through leaky vasculature [160,161]. A study by Harrington et al. [162] studied the biodistribution of ^{111}In-diethylenetriaminepentaacetic acid (^{111}In-DTPA) and compared it to ^{111}In-DTPA-labeled PEGylated liposomes (IDLPLs). The goal was to utilize polymerization with PEG to avoid breakdown from the RES and thus increase blood circulation time [162-164]. The results had shown a considerable increase in blood retention time and 10% of the injected dose was present in the blood for up to 96 hours whereas ^{111}In-DTPA was filtered below 10% circulating in the blood in less than 24 hours [162]. This is consistent with similar research into blood
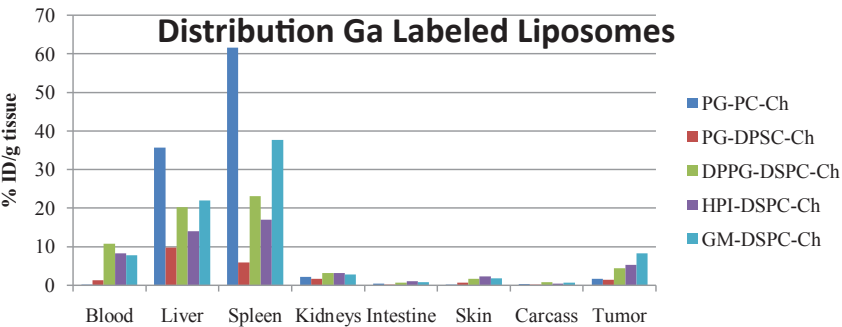
Figure 12: Distribution of liposomes with different functionalities 24 hours following IV injection. Data derived from previous research [156].
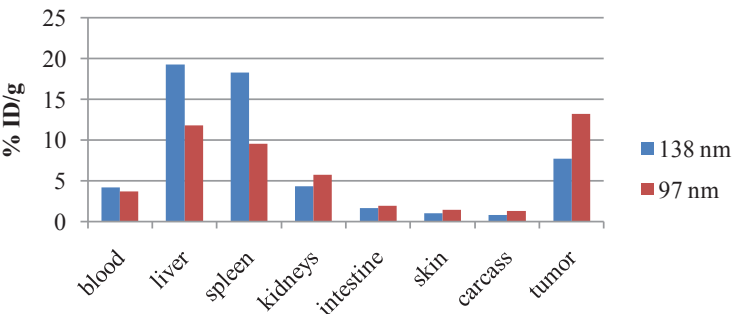

Figure 13: Distribution of 67Ga-labeled HPI-hydrogenated phosphatidylcholine (HPC)-Ch liposomes 24 post I.V. Data derived from previous research [165].
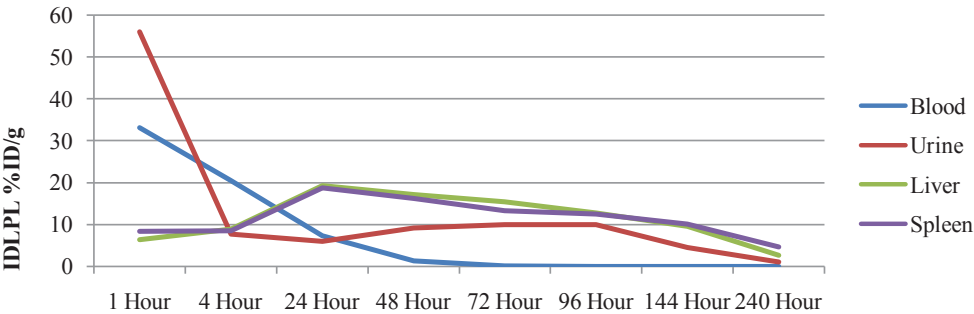

Figure 14: Retention time of IDLPL in the body over 240 hours post-IV injection. Data derived from previous research [163].
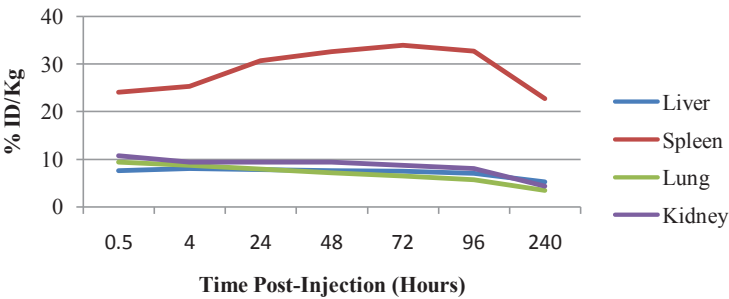

Figure 15: Uptake of IDLPL into different organs. Tissue weights were 1.6 kg (male liver), 1.3 kg (female liver), 0.15 kg (kidney) and 0.595 kg (lung). Data derived from previous research [164].

circulation time between IDLPL ^{111}In-DTPA [164]. The polymerized liposomes did see a clearance trend over time as can be seen in figure 14 that is consistent with the natural filtration of the excretory system.

Another study by Harrington et al. [161] analyzed organ uptake of IDLPL in human patients. His results verified uptake into tumors using IDLPL. The uptake into squamous cell cancer of the head and neck (SCCHN), lung tumors, and breast cancer tumors at 72 hours was 33 +/- 15.8, 18.3 +/- 5.7, and 5.3 +/- 2.6 % ID/kg organ weight, respectively [161]. The corresponding organ uptake can be seen in figure 15. The tissues had a significant uptake yet the tissues began to lower in concentration over time which is consistent with uptake by the excretory system. It was noticed in this experiment that there were no toxic effects to the patients with the exception of a single patient whose symptoms (incurred during administration) were abated within a few minutes after administration was arrested [161]. The symptoms did not reappear when the administration was continued under a slower rate [161].

A study by Paoli et al. [152] had shown the use of liposomes to increase blood retention time and tissue specificity. This is consistent with previous research which supports the need for prolonged blood retention time [156,164]. This study compared raw fluorophores, which are readily filtered out of the bloodstream (70% in the first hour), to liposome-encapsulated fluorophores [153]. The final liposome molecule (80-113 nm) was capable of released fluorophore in tumors at a 66-fold higher concentration than free drug after long circulation (24 hours post injection) [152].

This is, of course, reliant on prolonged blood retention time [30,156-164]. In a study by Dams et al. [163] an assessment of advanced filtration after multiple injections is done. The findings after multiple injections (one week between injections) of ^{99m}Tc-Hydrazinonicotinamide (HYNIC) PEG liposomes were that after the first injection the blood half-life was significantly reduced for the second and third injection.The blood half-life, however, began to increase again after the fourth injection as can be seen in figure 16 [163,165].

Blood circulation is not only controlled by injections and surface coatings, though. It has been shown in previous research that there are size constraints (70-300 nm in diameter) outside of which either the RES or the excretory system is initiated [166,167]. This is consistent with previous research denoting that the most functional use of nanoparticles for drug delivery is 20-200 nm [3]. It was reported, in a study by Kong et al. [166] (using 100, 200, and 400 nm liposomes) that extravasation into tissues decreased in liposomes as a function of increasing size. This decrease in extravasation was concluded to not be necessarily proportional to total administration of target drug because as the diameter of the liposome doubles the encapsulation volume increases up to an order of magnitude larger [168].

The final size-based limitations for liposomes were based on pore size for extravasation, which is different for different types of tumors. It was thus concluded that the particle diameter for optimal drug administration would be based on both tumor pore size and internal particle volume [24]. It was also noted that, aside from the RES and tumor, the 100 nm liposome group did not significantly accumulate in any tissue at normal body temperatures [169].

Another study by Harrington et al. [167] had tested different biodistributions of IDLPL in nude mice given different administration techniques. The patterns emerged that DTPA alone was unsuccessful at maintaining prolonged blood circulation as can be seen as the distribution differences between figures 17a and 17b. The subcutaneous injection of IDLPL was highly inefficiently cleared from the site of injection (Figure 17c) and noticed a proliferation of absorption into ipsilateral inguinal lymph node (IILN) to a peak of 57.9% injected dose/gram of tissue at 24 hours [167]. The biodistribution following an IV injection was more predictable and can be seen in (Figure 17d). The primary filtration post IV injection is immediately through the urine and then is filtered from the blood using the liver, likely through the RES, and temporarily agglomerates in the spleen [167].

A study by Menaa and Menaa [168] took a look into a novel liposomal encapsulation of mitotane, the only FDA approved chemotherapeutic drug for adreno-cortical carcinoma (ACC) [168-171]. There are many problems with mitotane including its natural hydrophobicity and high toxicity which can both be assisted by encapsulation within biocompatible and functionalized liposomes or lipid carriers [168,172,173]. There are two main types of lipid nanoparticles that can entrap molecules similar to liposomes and
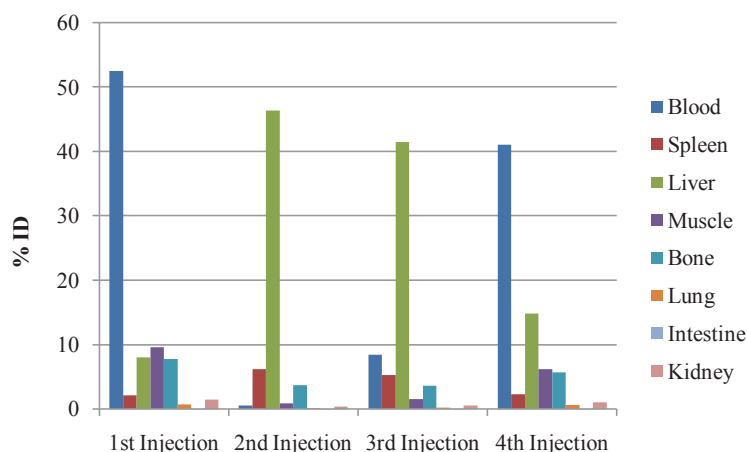

Figure 16: The biodistribution of ^{99m}Tc-labeled HYNIC PEGylated lyposomes at 4 hours post-injection. Injections were 1 week apart. Data derived from previous research [163].

offer different administration mediums. Solid lipid nanoparticles (SLN) are solid and carry the drug as either a homogenous mixture between the lipid structure and the drug, a shell that is enriched with the drug or a core that is drug-enriched [174]. SLNs offer an effective dispersion method as the nanoparticle can still administer the drug without having to be broken down first, unlike liposomes.

Nanostructured lipid carriers (NLC) are another type of lipid nanoparticle that offers unique benefits even above the SLNs. The benefits of NLCs and SLNs are that they are solid at body temperature, allowing for unique gastrointestinal uptake and allow for pharmaceutical applications [175,176]. NLCs have blends of solid and liquid lipids when made so the atomic structure is less perfect than that of SLNs. This allows for a larger payload per molecule
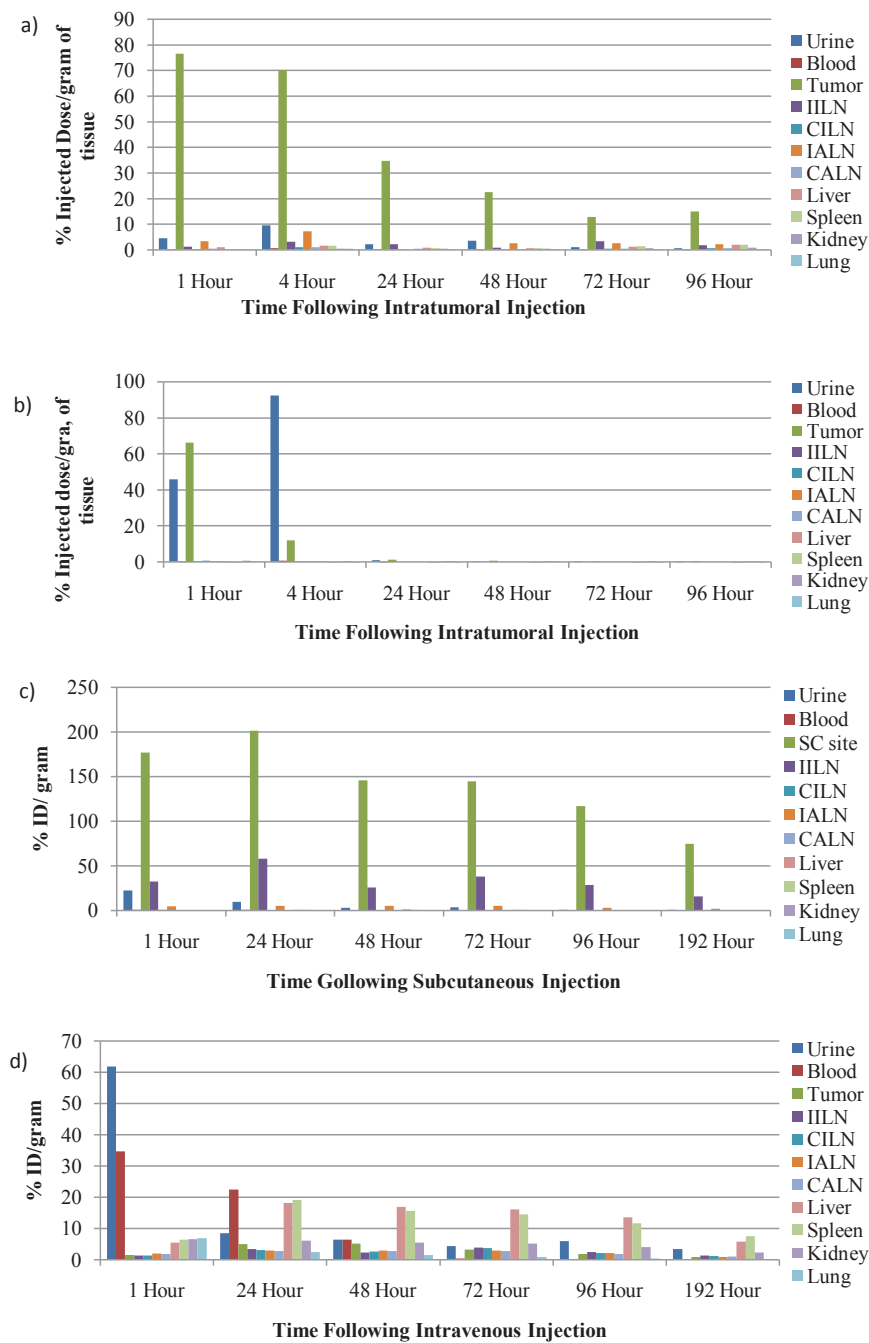

Figure 17: The biodistribution following different administration techniques in naked mole rats. a) IDLPL biodistribution following intratumoral injection, b) ^{111}In-DTPA distribution following intratumoral injection, c) IDLPL biodistribution following subcutaneous injection and d) IDLPL biodistribution following intravenous injection. Data derived from previous research [169].

Abbreviations: IILN: ipsilateral inguinal lymph node; IALN: ipsilateral axillary lymph node; CILN: contralateral inguinal lymph node; CALN: contralateral axillary lymph node.

and less expulsion of the active compound [168]. Both particles share the same biocompatibility as liposomes and follow similar pharmacokinetics yet NLCs and SLNs have longer stability [177].

In a study by Subbiah et al. [3] functionalized liposomes between 20 and 200 nm were considered optimal for drug delivery vessels. Molecules larger than 200 nm are readily degraded by the RES yet 5-100 nm liposomes did not elicit any type of immuno response. Previous research has shown that liposomes under 200 nm have significant extravasation into tumors [178-181] but other research proposes the most successful range of extravasation into tumors to be <100 nm, which of course varies depending on the type of tumor [3,168]. The smaller particles 5-100 nm go through the endocytotic pathway, which has a pH of 5.5, and the liposomes are degraded by lysosomal enzymes thus releasing the entrapped drug [25].

The biodistribution of liposomes post IV administration was largely determined by size and surface charge however the full distribution is also affected by the distance from functional ligand to NP, the binding strength of ligand and the total count of the ligand per NP [3]. It was also noted that PEG polymerization in particular increases blood circulation time and further reduces rapid RES clearance [181,182] and that cationic, as opposed to anionic, surface charge has a higher affinity to the cellular membrane [3].

Results

Oxidative stress is created naturally by ROS via neutrophils as part of the immune system and can initiate lipid peroxidation.This phenomenon can also be generated from in-vivo implementation of any particle if incorrectly prepared [46,47,54,56].

Depending on the required addition to the quantum dot particle, it can be a very powerful tool. This of course would not hold true if the diameter is less than 4 nm (they will be attacked by the immune system (Table 1)) [46] or near the micrometer scale (they will be engulfed by macrophages and degraded down to their toxic core) [53]. There is a useful size though, where tissue specificity is highly specialized and natural excretory systems are the main filtration medium. If the size is over 5.5 nm it can be filtered by the kidneys and liver and both ways under 3 days time which can be seen in table 1 [54].

Due to this ease of use and ability to elicit lipid peroxidation upon command, quantum dots are an extremely viable option for cancer treatments. Further work can be done to create further specificity from the quantum dots such that they are not only capable of being tissue-specific, including being specific to cancerous tissues, but also be able to pass the blood-brain barrier. This can be done by many changes including altering the surface chemistry via adding proteins.

Fullerenes are also powerful tools and if they are prepared in their water-soluble form, there was no reported attack by neutrophils even at their small diameter of less than 1 nm (0.71 nm) which can be seen in table 1. Although it was determined that the agglomeration in water led to an average unit size as 40-80 nm [182,183], it was noted that the in vivo agglomeration size was 1.8-2 nm (Table 1) [63]. Without being attacked by the immune system, they are also able to be passed through the body without a toxic effect [63,68]. It has also been proven that the specificity of fullerenes can be tailored such that in extreme cases of medication delivery they are able to be initiated via environmental factors specific to the tissue of interest [68]. This makes them otherwise non-toxic to the body in tissues not requiring medication.

Water soluble fullerene derivatives (C_3 being the best [40,60]) can be excellent radical scavengers throughout the body and even across the blood-brain barrier. Fullerenes have proven themselves to be the most capable particle for increasing reasoning functions over time and lengthening lifespan in mammals [60]. With the ease of administration and inability to elicit side-effects, this particle has extremely valuable possibilities.

Carbon nanotubes share the ability to be radical scavengers, but at the cost of being degraded over time. This is not unlike the degradation of fullerenes, but with an inability to be readily passed from the blood stream, degradation is more important in CNT usage than in fullerene usage. The inability of CNTs to be passed easily from the body is speculatively due to the unique shape of the nanotube (being a cylinder as opposed to a sphere) and its lack of hydrophilic functionalization frequently. These characteristics leave CNTs prone to becoming lodged in cellular membranes and agglomerating in the cytoplasm of cells causing cellular death.

Due to this phenomenon, nanotubes - if free in the body - have the potential to eventually cause extensive cellular death and maybe even loss of life in the patient. MWCNTs share this inability to be easily passed, as they are the same shape and surface chemistry. A possible solution could be forcibly keeping the CNTs from becoming aqueous in the body (like using them as an implanted scaffold for instance). This would change the function of them but as they are effectively a fullerene in cylinder form, the use of them has far more specialization as a surgical implant as opposed to an injected/ingested medication.

What is also important in CNTs is the choice between single-walled and multi-walled. The answer has been pretty clear that single-walled is commonly the better choice [89-91]. This is not only due to their greater conductivity and strength per unit volume and per unit weight but also because they have shown to elicit a lower toxic response from the body [89-91]. It is also important to perform purification tolerances on any sample being used in the medical field due to toxic impurities [8].

Nanodiamonds are subject to surface chemistry changes at low pH yet in vivo conditions only alter from its natural pH (~7.2) if inflammatory responses are seen [106]. They have been shown to be the least toxic of the nanocarbon materials as well [99]. In fact, the minimal existence of toxicity in NDs was seen only in a dose-dependen administration of agglomerated 40-100 nm particles which was lowered in the spleen and lung when larger particles were filtered out as can be seen in table 1 [110,111].

Diamondoids have a relatively low toxicity [99]. Whereas they are not spherical, their shape is cage-like which is significantly closer to spherical than CNTs. They are known to be readily cleared from the body when polar and capable of passing the blood-brain barrier at a size of 2-8 nm [105] (Table 1). A polar adamantane derivative known as memantine is on the order of ~1 nm [15] and is also known to be able to jump the blood-brain barrier and even have tissue specificity inside the brain [127]. These particles, like nanodiamonds are known to have the lowest toxic response of all the carbon nanomaterials (likely due to the inability for the body to break down the particles) [102]. Like the other carbon nanoparticles, not only are the small particles capable of jumping the blood-brain barrier but are safely eliminated from the body via normal excretory functions [126,127].

Gold is naturally non-polar and inert making it toxic in the body [128-131]. This seems, though, to be much more size dependent than one would initially think. 4, 12, and 18 nm sizes have been seen to pose no traces of toxicity and be able to be cleared by the body [129,130]. 1-2 nm particles have been seen to pose toxicity [129,130] (Table 1) yet appeared to have 77% of the injected particles cleared within 5 hours of administration [136]. It has also been seen that sizes up to 25 nm can clear the blood-brain barrier and that by raising the zeta potentials the distribution and clearance is much more predictable [132,134].

Silver particles are unique in that they are the only nanoparticle reviewed here that is favored to be filtered through solid waste over liquid waste [146,147]. This was most likely a byproduct of agglomeration due to a low zeta potential leading to larger particles that the body generally filters out via solid waste. The particles are known to have toxic effects to mitochondria if injected [140,149] which is likely due to an ability to elicit ROS throughout the body as a bi-product of the immune system's response to invasive and toxic particles [150].

Discussion

When comparing all of the above mentioned particles, trends begin to emerge. The most obvious trend is linked to administration technique. When administered intravenously, the nanoparticles have no option other than to agglomerate, be attacked, or be filtered out naturally yet when administered via ingestion techniques the larger particles never enter the blood stream. The natural filtration of the body's ingestion system is capable of selectively absorbing particles that are non toxic, as was seen with pharmaceutical uses of memantine, liposomes and C_{60} [24,26-38,42,107,108,153,154].

The strongest trends of the nanoparticles themselves is of size, shape and surface chemistry. If the particle is of a spherical shape, like liposomes, QDs or fullerenes, it is possible to pass it via the excretory system or the RES assuming it is within the predescribed size constraints. It is also possible to be non-spherical, like adamantane, yet cage-like and thus acts similar to spherical NPs inside the body.

In contrast, if it is not a spherical or cage-like, like CNTs, and is large it will have many difficulties travelling through the blood. At this point it can become aggressively lodged in the membranes of tissues and cells similar to if one were to try to pass a pencil down a tube filled with moving water balloons. It would be nearly impossible to get the pencil from one end to another (assuming the tube is sufficiently long, let's say one meter) without the pencil penetrating the exterior of at least one balloon. This could only be avoided if the pencil was sufficiently short so as to be closer to a cage-like formation than a stiff nanorod.

The last primary attribute to assess is the chemistry of the particle in question. If any particle is non-polar, it will agglomerate and either adsorb onto tissues or be attacked by the immune system. It is also known that a greater zeta potential helps to fight agglomeration (~30 mV appears to be the cutoff between high agglomeration and dissociation) [135]. If it is polar, then the next assessment is of the core makeup of the particle. Depending on the type of nanoparticle, the size related distribution is particular to the material in question (Table 1). The core makeup of the particles is relative to the natural filtration. If the nanoparticle core is non-toxic and biocompatible

it will have a larger size distribution than those which are naturally toxic.

When particles such as silver nanoparticles are released into the body, they have low zeta potentials and thus are capable of agglomerating and being attacked by the immune system in a non-filtrating way. This creates a toxic environment for blood cells before a portion of the nanoparticles are eliminated via solid waste. This happens even though the particles begin at a very small diameter.

As for fullerenes, and other nanomaterials that are spherical and carbon-based, size is still important as the functional coating must not be too large. If the polar end is too far from the core, the particle can begin to take on a different shape other than a sphere and thus have problems traversing the blood stream. On the same note, if the polar end is in charge of accomplishing the medication parameters, if it is too long itself the shape of the particle will no longer be a sphere and the problems associated with the nanotubes will begin to take place.

References

1. Vahabi K, Mansoori GA, Karimi S (2011) Biosynthesis of silver nanoparticles by fungus *Trichoderma reesei* (a route for large-scale production of AgNPs). Insciences J 1: 65-79.

2. Mansoori GA (2002) Advances in atomic & molecular nanotechnology. Nanotech, United Nations Tech Monitor 53.

3. Subbiah R, Veerapandian M, Yun KS (2010) Nanoparticles: Functionalization and multifunctional applications in biomedical sciences. Curr Med Chem. 17:4559-4577.

4. Menaa B (2011) The importance of nanotechnology in biomedical sciences. J Biotech Biomat 1: 5.

5. Vakili-Nezhaad GR, Mansoori GA, Ashrafi AR (2007) Symmetry property of fullerenes. Journal of Computational and Theoretical Nanoscience 4: 1202-1205.

6. Nazem A, Mansoori GA (2011) Nanotechnology for Alzheimer's disease detection and treatment. Insciences J 1: 169-193.

7. Nazem A, Mansoori GA (2008) Nanotechnology solutions for Alzheimer's disease: advances in research tools, diagnostic methods and therapeutic agents. J Alzheimers Dis 13: 199-223.

8. Tejral G, Panyala NR, Havel J (2009) Carbon nanotubes: toxicological impact on human health and environment. Applied Biomedicine 7: 1-13.

9. Sabzyan H, Tavangar Z (2009) Characterization of the flow of the CO/CO_2 gases through carbon nanotube junctions using molecular dynamic simulations. Chemical Physics 362: 120-129.

10. Mohazzabi P, Mansoori GA (2006) Why Nanosystems and Macroscopic Systems Behave Differently. Int J Nanoscience & Nanotech 1: 46-53.

11. Ramezani H, Mansoori GA, Saberi MR (2007) Diamondoids-DNA nanoarchitecture: From nanomodules design to self-assembly. J Computational and Theoretical Nanoscience 4: 96-106.

12. Ramezani H, Mansoori G (2007) Diamondoids as molecular building blocks for nanotechnology. Molecular Building Blocks for Nanotech 109: 44-71.

13. Xue Y, Mansoori GA (2010) Self-assembly of diamondoid molecules and derivatives (MD simulations and DFT calculations). Int J Mol Sci 11: 288-303.

14. Keshavarzi T, Sohrabi R, Rezvan, Mansoori GA (2006) An analytic model for nano confined fluids phase-transition: applications for confined fluids in nanotube and nanoslit. J Computational and Theoretical Nanoscience 3: 134-41.

15. Yong X, Mansoori GA (2008) Quantum Conductance and Electronic Properties of Lower Diamondoid Molecules and Derivatives. Int J Nanoscience 7: 63-72.

16. Zhang, GP, George TF, Assoufid L, Mansoori GA (2007) First-principles

simulation of the interaction between adamantane and an atomic-force-microscope tip. Phys Rev B 75: 035413.

17. Shakeri-Zadeh A, Mansoori GA, Hashemian AR, Eshghi H, SazgarniaA, et al. (2010) Cancerous Cells Targeting and Destruction Using Folate Conjugated Gold Nanoparticles. Dyn Biochem Process Biotechnol Mol Biol 4: 6-12.

18. Mansoori GA, Brandenburg KS, Shakeri-Zadeh A (2010) A Comparative Study of Two Folate-Conjugated Gold Nanoparticles for Cancer Nanotechnology Applications. Cancers 2: 1911-1928.

19. Shakeri-Zadeh A, Mansoori GA (2010) Cancer Nanotechnology Treatment through Folate Conjugated Gold Nanoparticles. Proceedings of WCC 2010 (The 2nd World Congress on Cancer).

20. Mansoori GA, Mohazzabi P, McCormack P, Jabbari S (2007) Nanotechnology in cancer prevention, detection and treatment: bright future lies ahead. World Review of Science, Technology and Sustainable Development 4: 226-257.

21. Hashemian A, Eshghi H, Mansoori GA, Shakeri-Zadeh A, Mehdizadeh A "Folate-conjugated gold nanoparticles. Synthesis, characterization and design for cancer cells nanotechnology-based targeting". International Journal of Nanoscience and Nanotechnology.

22. Brandenburg KS, Shakeri-Zadeh A, Mansoori GA (2011) Folate-Conjugated Gold Nanoparticles for Cancer Nanotechnology Applications. Nanotech 3 Proceedings: 404-407.

23. Shakeri-Zadeh A, Eshghi H, Mansoori GA, Hashemian AR (2009) Gold Nanoparticles Conjugated with Folic Acid using Mercaptohexanol as the Linker. J Nanotech Progress Internat *(JONPI)* 1: 13-23.

24. Mansoori GA (2010) Synthesis of nanoparticles by fungi. U.S. Patent Application 12/511,800.

25. Osada K, Christie RJ, Kataoka K (2009) Polymeric micelles from poly(ethylene glycol)-poly(amino acid) block copolymer for drug and gene delivery. J R Soc Interfac 6: S325-S339.

26. Safra T, Muggia F, Jeffers S, Tsao-Wei DD, Groshen S, et al. (2000) Pegylated liposomal doxorubicin (doxil): Reduced clinical cardiotoxicity in patients reaching or exceeding cumulative doses of 500 mg/m(2). Ann Oncol 11:1029–1033.

27. Yildirim Y, Gultekin E, Avci ME, Inal MM, Yunus S, et al. (2008) Cardiac safety profile of pegylated liposomal doxorubicin reaching or exceeding lifetime cumulative doses of 550 mg/m(2) in patients with recurrent ovarian and peritoneal cancer. Int J Gynecol Cancer 18: 223–227.

28. Olson F, Mayhew E, Maslow D, Rustum Y, Szoka F (1982) Characterization, toxicity and therapeutic efficacy of adriamycin encapsulated in liposomes. Eur J Cancer Clin Oncol 18: 167-169.

29. Gregoriades G, Swain CP, Wills EJ, Tavill AS (1974) Drug-carrier potential of liposomes in cancer chemotherapy. Lancet. 1: 1313-1316.

30. Allen TM, Chonn A (1987) Large unilamellar liposomes with low uptake by the reticuloendothelial system. FEBS Lett. 223: 42-6.

31. Gabizon A, Papahadjopoulos D (1988) Liposome formulations with prolonged circulation time in blood and enhanced uptake in tumors. Proc Natl Acad Sci USA 85:6949-6953.

32. Papahadjopoulos D, Allen TM, Gabizon A, Mayhew E, Matthay K, et al. (1991) Sterically stabilized liposomes: improvements in pharmacokinetics and antitumor therapeutic efficacy. Proc Natl Acad Sci USA 88: 11460-11464.

33. Harrison M, Tomlinson D, Stewart S (1995) Liposomal entrapped doxorubicin: an active agent in AIDS-related Kaposi's sarcoma. J Clin Oncol 13: 914-920.

34. Goebel FD, Goldstein D, Goos M, Jablonowski H, Stewart JS (1996) Efficacy and safety of Stealth liposomal doxorubicin in AIDS-related Kaposi's Sarcoma. Br J Cancer 73:989-994.

35. Northfelt DW, Dezube B, Thommes JA, Miller BJ, Fischl MA, et al. (1998) Pegylated-liposomal doxorubicin versus doxorubicin, bleomycin and vincristine in the treatment of aids-related Kaposi's sarcoma: results of a randomised phase III clinical trial. J Clin Oncol 16: 2445-2451.

36. Stewart JSW, Jablonowski H, Goebel FD, Arasteh K, Spittle M, et al. (1998) Randomised comparative trial of pegylated liposomal doxorubicin versus bleomycin and vincristine in the treatment of AIDS-related Kaposi's sarcoma. International Pegylated Liposomal Doxorubicin Study Group. J Clin Oncol 16: 683-691.

37. Muggia FM, Hainsworth JD, Jeffers S, Miller P, Groshen S, et al. (1997) Phase II study of liposomal doxorubicin in refractory ovarian cancer: antitumor activity and toxicity modification by liposomal encapsulation. J Clin Oncol 15: 987-993.

38. Ranson MR, Carmichael J, O'Byrne K, Stewart S, Smith D, et al. (1997) Treatment of advanced breast cancer with sterically stabilized liposomal doxorubicin: results of a multicentre phase II trial. J Clin Oncol 15: 3185-3191.

39. Dreher KL (2004) Health and environmental impact of nanotechnology: toxicological assessment of manufactured nanoparticles. Toxicol Sci 77: 3-5.

40. Wang IC, Tai LA, Lee DD, Kanakamma PP, Shen CKF, et al. (1999) C60 and Water-Soluble Fullerene Derivatives as Antioxidants Against Radical-Initiated Lipid Peroxidation. J Med Chem 42: 4614-4620.

41. Tsay JM, Trzoss M, Shi L, Kong X, Selke M, et al. (2007) Singlet Oxygen Production by Peptide-coated Quantum Dot-Photosensitizer Conjugates. J Amer Chem Soc 129: 6865-6871.

42. Juzenas P, Chen W, Sun YP, Coelho MAN, Generalov R, et al. (2008) Quantum dots and nanoparticles for photodynamic and radiation therapies of cancer. Adv Drug Deliv Rev 60: 1600-1614.

43. Gao X, Cui Y, Levenson RM, Chung LWK, Nie S (2004) *In vivo* cancer targeting and imaging with semiconductor quantum dots. Nature Biotech 22: 69-976.

44. Michalet X, Pinaud FF, Bentolila LA, Tsay JM, Doose S, et al. (2005) Quantum Dots for Live Cells, *in vivo* Imaging, and Diagnostics. Science 307: 538-544.

45. Liu W, Choi HS, Zimmer JP, Tanaka E, Frangioni JV, et al. (2007) Compact Cysteine-Coated CdSe(ZnCdS) QDs for *In vivo* Applications. J Am Chem Soc 129: 14530-14531.

46. Smith AM, Duan H, Mohs AM, Nie S (2008) Bioconjugated Quantum Dots for *In vivo* Molecular and Cellular Imaging. Adv Drug Deliv Rev 60: 1226-1240.

47. Su Y, Peng F, Jiang Z, Zhong Y, Lu Y, et al. (2011) *In vivo* distribution, pharmacokinetics, and toxicity of aqueous synthesized cadmium-containing quantum dots. Biomaterials 32: 5855-5862.

48. Derfus AM, Chan WCW, Bhatia SN (2004) Probing the cytotoxicity of semiconductor quantum dots. Nano Lett 4: 11-8.

49. Kirchner C, Liedl T, Kudera S, Pellegrino T, Munox Javier A, et al. (2005) Cytotoxicity of colloidal CdSe and CdSe/ZnS nanoparticles. Nano Lett 5: 331-338.

50. Schipper ML, Iyer G, Koh AL, Cheng Z, Ebenstein Y, et al. (2009) Particle size, surface coating, and PEGylation influence the biodistribution of quantum dots in living mice. Small 5: 126-134.

51. Daou TJ, Li L, Reiss P, Josserand V, Texier I (2009) Effect of poly(ethylene glycol) length on the *in vivo* behavior of coated quantum dots. Langmuir 25: 3040-3044.

52. Chithrani BD, Ghazani AA, Chan WC (2006) Determining the size and shape of dependence of gold nanoparticle uptake into mammalian cells. Nano Lett 6: 662-668.

53. Choi HS, Liu W, Misra P, Tanaka E, Zimmer JP, et al. (2007) Renal clearance of Nanoparticles. Nat Biotech 25: 2265-2270.

54. Choi HS, Ipe BI, Misra P, Lee JH, Bawendi MG, et al. (2009) Tissue- and Organ-Selective Biodistribution of NIR Fluorescent Quantum Dots. Nano Lett 9: 2354-2359.

55. Cheng TF, Sun YD, Si DY, Liu CX (2009) Attention on research of pharmacology and toxicology of nanomedicines. Asian J Pharmacodynamics and Pharmacokinetics 9: 27-49.

56. Baker GL, Gupta A, Clark ML, Valenzuela BR, Staska LM, et al. (2008) Inhalation Toxicity and Lung Toxicokinetics of C60 Fullerene. Nanoparticles and Microparticles. Toxicol Sci 101: 122-131.

57. Gupta A, Forsythe WC, Clark ML, Dill JA, Baker GL (2007) Generation of C60 nanoparticle aerosols in high mass concentrations. J Aerosol Sci 38: 582-603.

58. Beuerle F, Lebovitz R, Hirsch A (2008) Antioxidant properties of water-soluble fullerene derivatives. Med Chem and Pharmacol Potential of Fullerenes and Carbon Nanotubes 51-78.

59. Sayes CM, Gobin AM, Ausman KD, Mendez J, West JL, et al. (2005) Nano-C_{60} cytotoxicity is due to lipid peroxidation. Biomaterials 26: 7587-7595.

60. Dugan LL, Turetsky DM, Du C, Lobner D, Wheeler M, et al. (1997) Carboxyfullerenes as neuroprotective agents. Proc Natl Acad Sci USA 94: 9434-9439.

61. Belyanskaya L, Weigel S, Hirsch C, Tobler U, Krug HF, et al. (2009) Effects of carbon nanotubes on primary neurons and glial cells Neurotoxicology 30: 702-711.

62. Vlasova II, Vakhrusheva TV, Sokolov AV, Kostevich VA, Ragimov AA (2011) Peroxidase-induced degradation of single-walled carbon nanotubes: hypochlorite is a major oxidant capable of *in vivo* degradation of carbon nanotubes. J Phys Conf Ser 291.

63. Boushehri SVS, Ostad SN, Sarkar S, Kuznetsov DA, Buchachenko AL, et al. (2010) The C60-Fullerene Porphyrin Adducts for Prevention of the Doxorubicin-Induced Acute Cardiotoxicity in Rat Myocardial Cells. Acta Med Iran 48: 342-350.

64. Wallace KB, Starkov AA (2000) Mitochondrial targets of drug toxicity. Annu Rev Pharmacol Toxicol 40: 353-388.

65. Tien M, Svingen BA, Aust SD (1982) AnInvestigation into the Role of Hydroxyl Radical in Xanthine Oxidase-Dependent Lipid Peroxidation. Arch Biochem Biophys 216: 142-151.

66. Fukuzawa K, Tadakero T, Kishikawa K, Mukai K, Gebicki JM (1988) Site Specific Induction of Lipid Peroxidation by Iron in Charged Micelles. Arch Biochem Biophys 260: 146-152.

67. Gutteridge JM (1982) The Role of Superoxide and Hydroxyl Radicals in Phospholipid Peroxidation Catalyzed by Iron Salts. FEBS Lett. 150: 454-458.

68. Quick KL, Ali SS, Arch R, Xiong C, Wozniak D, et al. (2008) A carboxyfullerene SOD mimetic improves cognition and extends the lifespan of mice. Neurobiol Aging 29: 117-128.

69. Schriner SE, Linford NJ, Martin GM, Treuting P, Ogburn CE, et al. (2005) Extension of murine life span by overexpression of catalase targeted to mitochondria. Science 308: 1909–1911.

70. Sayes CM, Fotner JD, Guo W, Lyon D, Boyd AM, et al. (2004) The differential cytotoxicity of water-soluble fullerenes. Nano Lett 4: 1881-1887.

71. Bellush LL, Wright AM, Walker JP, Kopchick J, Colvin RA (1996) Caloric restriction and spatial learning in old mice. Physiol Behav 60: 541–547.

72. Mazatenta A, Giuliano M, Campidelli S, Gambazzi L, Businaro L, et al. (2007) Interfacing Neurons with Carbon Nanotubes: Electrical Signal Transfer and Synaptic Stimulation in Cultured Brain Circuits. J Neurosci 27: 6931-6936.

73. Shein M, Greenbaum A, Gabay T, Sorkin R, David-Pur M, et al. (2008) Engineered neuronal circuits shaped and interfaced with carbon nanotube microelectrode arrays. Biomed Microdevices 11: 495-501.

74. Alessandri-Haber N, Paillart C, Arsac C, Gola M, Couraud F, et al. (1999) Specific distribution of sodium channels in axons of rat embryo spinal motoneurones. J Physiol 518: 203-214.

75. Fiorito S, Serafino A, Andreola F, Bernier P (2006) Effects of fullerenes and single-walled carbon nanotubes on murine and human macrophages. Carbon 44: 1100-1105.

76. Murad F (1999) Discovery of some of the biological effects of nitric oxide and its role in cell signaling. Biosci Rep 24: 452-474.

77. Lowenstein CJ, Dinerman JL, Snyder SH (1994) Nitric oxide: a physiologic messenger. Ann Intern Med 120: 227-37.

78. Anderson RS, Thomson SM, Gutshall LL Jr (1989) Comparative effects of inhaled silica or synthetic graphite dusts on rat alveolar cells. Arch Environ Contam Toxicol 18: 844-849.

79. Eriksson C, Nygren H (1997) The initial reaction of graphite and gold with blood. J Biomed Mater Res 37: 130-136.

80. Liang G, Yin L, Zhang J, Liu R, Zhang T, et al. (2010) Effects of Subchronic Exposure to Multi-Walled Carbon Nanotubes on Mice. J Toxicol Environ Health A 73: 463-470.

81. Schipper M L, Nakayama-Ratchford N, Davis CR, Kam NWS, Chu P, et al. (2008) A pilot toxicology study of single-walled carbon nanotubes in a small sample of mice. Nat Nanotech 3: 216-221.

82. Dent X, Jia G, Wang H, Sun H, Wang X, et al. (2007) Translocation and fate of multi-walled carbon nanotubes *in vivo*. Carbon 45: 1419-1424.

83. Deng X, Wu F, Liu Z, Luo M, Li L, et al. (2009) The splenic toxicity of water soluble multi-walled carbon nanotubes in mice. Carbon 47: 1421-1428.

84. Yang X, Guo Q, Lin Y, Deng X, Wang H, et al. (2007) Biodistribution of pristine single-walled carbon nanotubes *in vivo*. J Phys Chem C 111: 17761-17764.

85. Liu Z, Davis C, Cai WB, He L, Chen X, et al. (2008) Circulation and long-term fate of functionalized, biocompatible single-walled carbon nanotubes in mice probed by raman spectroscopy. Proc Natl Acad Sci USA 105: 1410-1415.

86. Hirano S, Kanno S, Furuyama A (2008) Multi-walled carbon nanotubes injure the plasma membrane of macrophages. Toxicol Appl Pharmacol 232: 244-251.

87. Fubini B, Hubbard A (2003) Reactive oxygen species (ROS) and reactive nitrogen species (RNS) generation by silica in inflamation and fibrosis. Free Radic Bio Med 34: 1507-1516.

88. Hussain S, Boland S, Baeza-Squiban A, Hamal R, Thomassen LC, et al. (2009) Oxidative stress and proinflammatory effects of carbon black and titanium dioxide nanoparticles: role of particle surface area and internalized amount. Toxicology 260: 142-149.

89. Park EJ, Park K (2009) Oxidative stress and pro-inflammatory responses induced by silica nanoparticles *in vivo* and *in vitro*. Toxicol Lett 184:18-25.

90. Lam CW, James JT, McCluskey R, Hunter RL (2004) Pulmonary toxicity of single-wall carbon nanotubes in mice 7 and 90 days after intratracheal instillation. Toxicol Sci 77: 126-134

91. Warheit DB, Laurence BR, Reed KL, Roach DH, Reynolds GA, et al. (2004) Comparative pulmonary toxicity assessment of single-wall carbon nanotubes in rats. Toxicol Sci 77: 117-125.

92. Allen BL, Kotchey GP, Chen Y, Yanamala NV, Klein-Seetharaman J, et al. (2009) Mechanistic investigations of horseradish peroxidase-catalyzed degradation of single-walled carbon nanotubes. J Am Chem Soc 131: 17194-17205.

93. Kagan VE, Konduru NV, Feng W, Allen BL, Conroy J, et al. (2010) Carbon nanotubes degraded by neutrophil myeloperoxidase induce less pulmonary inflammation. Nat Nanotechno l5: 354-359.

94. Klebanoff SJ (2005) Myeloperoxidase: friend and foe. J Leukoc Biol 77: 598-625.

95. Vlasova II, Chekanov AV, Matskevich VA, Sokolov AV (2009) Biodegradation of single-walled carbon nanotubes by leucocytic myeloperoxidase. Abstract Book of II Nanotechnology International forum, Moscow 603-605.

96. Liu Z, Chen K, Davis C, Sherlock S, Cao Q, et al. (2008) Drug delivery with carbon nanotubes for *in vivo* cancer treatment. Cancer Res 68: 6652-6660.

97. Zhao B, Hu H, YA, Perea D, Haddon RC (2005) Synthesis and characterization of water soluble single-walled carbon nanotube craft copolymers. J Am Chem Soc 127: 8197-203.

98. Maynard AD, Baron PA, Foley M, Shvedova AA, Kisin ER, et al. (2004) Exposure to carbon nanotube material: Aerosol release during the handling of unrefined single-walled carbon nanotube material. J Toxicol Environ Health Part A 67: 87–100.

99. Davboren M, Herzog E, Casey A, Cottineau B, Chambers G, et al. (2007) *In vitro* toxicity evaluation of single-walled carbon nanotubes on human A549 lung cells. Toxicol *In vitro* 21: 438-448.

100. Diabeté S, Mülhopt S, Paur HR, Wottrich R, Krug HF (2004) *In vitro* effects of incinerator fly ash on pulmonary macrophages and epithelial cells. Internat J of Hyg Environ Health 204: 323–326.

101. Shvedova AA, Castranova V, Kisin ER, Schwegler-Berry D, Murray AR, et al. (2003) Exposure to carbon nanotubes material: assessment of nanotubes cytotoxicity using human keratinocyte cells. J Toxicol Environ Health A 66: 1909-1926.

102. Wörle-Knirsch JM, Pulskamp K, Krug HF (2006) Oops they did it again! Carbon nanotubes hoax scientists in viability assays. Nano Lett 6: 1261-1268.

103. Pulskamp K, Wörle-Knirsch JM, Hennrich F, Kern K, Krug HF (2007) Human lung epithelial cells show biphasic oxidative burst after single-walled carbon nanotube contact. Carbon 45: 2241-2249.

104. Pulskamp K, Diabate S, Harald F, Krug HF (2007) Carbon nanotubes show no sign of acute toxicity but induce intracellular reactive oxygen species in dependence on contaminants. Toxicol Lett 168: 58-74.

105. Zhu Y, Li J, Li W, Zhang Y, Yang X, et al. (2012) The Biocompatibility of Nanodiamonds and Their Application in Drug Delivery Systems. Theranostics 2: 302-312.

106. Neugart F, Zappe A, Jelezko F, Tietz C, Boudou JP, et al. (2007) Dynamics of diamond nanoparticles in solution and cells. NanoLetters 7: 3588-3591.

107. Yuan Y, Wang X, Jia G, Liu JH, Wang T, et al. (2010) Pulmonary toxicity and translocation of nanodiamond in mice. Diam Relat Mater. 19: 291-299.

108. Muller L, Huaux F, Moreau N, Misson P, Heilier JF, et al. (2005) Respiratory toxicity of multi-wall carbon nanotubes. Toxicol Appl Pharmacol 207: 221-231.

109. Schrand AM, Hens SAC, Shenderova OA (2009) Nanodiamond particles: properties and perspectives for bioapplications. Crit Rev Solid State 34: 18-74.

110. Zhang XY, Yin J, Cheng K, Li J, Zhu Y, et al. (2010) Biodistribution and toxicity of nanodiamonds in mice after intratracheal instillation. Toxicol Lett. 198: 237-243.

111. Yuan Y, Chen YW, Liu JH, Wang H, Liu Y (2009) Biodistribution and fate of nanodiamonds *in vivo*. Diamond Relat Mater 18: 95-100.

112. Rojas S, Gispert JD, Martin R, Abad S, Menchon C, et al. (2011) Biodistribution of amino-functionalized diamond nanoparticles. *In vivo* studies based on 18F radionuclide emission. ACS Nano 5: 5552-5559.

113. Chow EK, Zhang XQ, Chen M, Lam R, Robinson E, et al. (2011) Nanodiamond therapeutic delivery agents mediate enhanced chemoresistant tumor treatment. Sci Transl Med 3: 73.

114. Pun SH, Bellocq NC, Liu A, Jensen G, Machemer T, et al. (2004) Cyclodextrin-Modified Polyethylenimine Polymers for Gene Delivery. Bioconjug Chem 15:831- 840.

115. Fu CC, Lee HY, Chen K, Lim TS, Wu HY, et al. (2007) Characterization and application of single fluorescent nanodiamonds as cellular biomarkers. Proc Natl Acad Sci USA 104: 727-732.

116. Yang W, Auciello O, Butler JE, Cai W, Carlisle JA, et al. (2002) DNA-modified nanocrystalline diamond thin-films as stable, biologically active substrates. Nat Mater 1: 253-257.

117. Parsons CG, Gruner R, Rozental J, Millar J, Lodge D (1993) Patch clamp studies on the kinetics and selectivity of NMDA receptor antagonism by memantine. Neuropharmacol 32: 1337-1350.

118. Danielczyk W (1995) Twenty-five years of amantadine therapy in Parkinson's disease. J Neural Transm Suppl 46: 399–405.

119. Jackish R, Link T, Neufang B, Koch R (1992) Studies on the mechanism of action of the antiparkinsonian drugs memantine and amantadine: no evidence for direct opaminergic or antimuscurinic properties. Arch Int Pharmacodyn Ther 320: 21-42.

120. Oxford J S, Galbraith A (1980) Antiviral activity of amantadine: a review of laboratory and clinical data. Pharmacol Ther 11:181–262.

121. Francis PT (2008) Glutamatergic approaches to the treatment of cognitive and behavioural symptoms of Alzheimer's disease. Neurodegener Dis 5:241–243.

122. Bormann J (1989) Memantine is a potent blocker of N-methyl-D-aspartate (NMDA) receptor channels. Eur J Pharmacol 166 591-592.

123. Chen HS, Pellegrini JW, Aggarwal SK, Lei SZ, Warach S, et al. (1992) Open channel block of N-methyl-D-aspartate (NMDA) responses by memantine: therapeutic advantage against NMDA receptor-mediated nuerotoxicity. J Neurosci 12: 4427-4436.

124. Samnick S, Ametamey S, Leenders KL, Vontobel P, Quack G, et al. (1998) Electrophysiological study, biodistribution in mice, preliminary PET evaluation in a rhesus monkey of 1-amino-3-[^{18}F]fluoromethyl-5methyl-adamantane (^{18}F-MEM): a potential radioligand for mapping the NMDA-receptor complex. Nuclear Med Bio 25:323-330.

125. Ametamey SM, Bruehlmeier M, Kneifel S, Kokic M, Honer M, et al. (2001) PET studies of ^{18}F-memantine in healthy volunteers. Nuclear Med Biol 29: 227-231.

126. Amiji M, Park K (1992) Prevention of protein adsorption and platelet adhesion on surfaces by PEO/PPO/PEO triblock copolymers. Biomater 13:682-692.

127. Davis SS, Washington C, West P, Illum L, Liversidge G, et al. (1987) Lipid emulsions as drug delivery systems. Ann N Y Acad Sci 507: 75-88.

128. Connor EE, Mwamuka J, Gole A, Murphy CJ, Wyatt MD (2005) Gold nanoparticles are taken up by human cells but do not cause acute cytotoxicity. Small 1: 325–327.

129. Moghimi SM, Porter CJH, Muir IS, Illum L, Davis SS (1991) Non-phagocytic uptake of intravenously injected microspheres in rat spleen: influence of particle size and hydrophilic coating. Biochem Biophys Res Commun 177: 861-866.

130. Guerrero S, Herance JR, Jojas S, Mena JF, Gispert JD, et al. (2012) Synthesis and *in vivo* Evaluation of the Biodistribution of a 18F-Labeled Conjugate Gold-Nanoparticle-Peptide with Potential Biomedical Application. Bioconjug Chem 23: 399-408.

131. Sonavane G, Tomoda K, Makino K (2008) Biodistribution of colloidal gold nanoparticles after intravenous administration: effect of particle size. Colloids Surf B Biointerfaces 66: 274-280.

132. De Jong WH, Hagens WI, Krystek P, Burger MC, Sips AJ, et al. (2008) Particle size-dependent organ distribution of gold nanoparticles after intravenous administration. Biomaterials 29:1912-1919.

133. Stolnik S, Illum L, Davis SS (1995) Long circulating microparticulate drug carriers. Advanced Drug Deliv Rev 16: 195-214.

134. Huber M, Wei TF, Muller UR, Lefebvre PA, Marla SS, et al. (2004) Gold nanoparticle probe-based gene expression analysis with unamplified total human RNA. Nucleic Acids Res 32: e137.

135. Bihari P, Vippola M, Schultes S, Praetner M, Khandoga AG, et al. (2008) Optimized dispersion of nanoparticles for biological *in vitro* and *in vivo* studies. Part Fibre Toxicol 5:14.

136. Niidome T, Yamagata M, Okamoto Y, Akiyama Y, Takahashi H, et al. (2006) PEG-modified gold nanorods with a stealth character for *in vivo* applications. J Control Release 114: 343-347.

137. Lok CN, Ho CM, Chen R, He QY, Yu WY, et al. (2007) Silver nanoparticles: partial oxidation and antibacterial activities. J Biol Inorg Chem 12:527-534.

138. Kone BC, Kaleta M, Gullans SR (1988) Silver ion (Ag$^+$) induced increases in cell membrane K$^+$ and Na$^+$ permeability in renal proximal tubule: reversal by thiol reagents. J Membr Biol 102: 11-19.

139. Chen X, Schluesener HJ (2008) Nanosilver: A nanoproduct in medical application. Toxicol Lett 176:1-12.

140. Kim YS, Kim JS, Cho HS, Rha DS, Kim JM, et al. (2008) Twenty-Eight-Day Oral Toxicity, Genotoxicity, and Gender-Related Tissue Distribution of Silver Nanoparticles in Sprague-Dawley Rats. Inhal Toxicol 20: 575-583.

141. Tang J, Xiong L, Wang S, Wang J, Liu L, et al. (2009) Distribution, Translocation and Accumulation of Silver Nanoparticles in Rats. J Nanosci Nanotechnol 9: 4924-4932.

142. Loeschner K, Hadrup N, Qvortrup K, Larsen A, Gao X, et al. (2011) Distribution of silver in rats following 28 days of repeated oral exposure to silver nanoparticles or silver acetate. Part Fibre Toxicol 8: 8-18.

143. Garza-Ocañas L, Ferrer DA, Burt J, Diaz-Torres LA, Ramírez Cabrera M, et al. (2010) Biodistribution and long-term fate of silver nanoparticles functionalized with bovine serum albumin in rats. Metallomics 2: 204-210.

144. ATSDR (1999) Toxicological Profile for Silver. Agency for Toxic Substances and Disease Registry, U.S. Department of Health and Human Services, Public Health Service.

145. Gregus Z, Klaassen CD (1986) Disposition of metals in rats: A comparative study of fecal, urinary, and biliary excretion and tissue distribution of eighteen metals. Toxicol Appl Pharmacol 85: 24-38.

146. Klaassen CD (1979) Biliary excretion of silver in the rat, rabbit, and dog. Toxicol Appl Pharmacol 50: 49-55.

147. Chappell JB, Greviller GD (2954) Effect of silver ions on mitochondrial adenosine triphosphatase. Nature 174:930-931.

148. Alfmofti MR, Ichikawa T, Yamashita K, Terada H, Shinohara Y (2003) Silver ion induces a cyclosporine a-insensitive permeability transition in rat liver mitochondria and release of apoptogenic cytochrome C. J Biochem 134: 43-49.

149. Nel A (2005) Atmosphere. Air pollution-related illness: effects of particles. Science 308: 804-806.

150. Elechiguerra JL, Burt JL, Morones JR, Camacho-Bragado A, Gao X, et al. (2005) Interaction of silver nanoparticles with HIV-1. J Nanobiotech 3: 6.

151. Morones JR, Elechiguerra JL, Camacho A, Holt K, Kouri JB, et al. (2005) The bactericidal effect of silver nanoparticles. Nanotech 16: 2346-2353.

152. Paoli EE, Kruse DE, Seo JW, Zhang H, Kheirolomoom A, et al. (2010) An optical and microPET assessment of thermally-sensitive liposome biodistribution in the Met-1 tumor model: importance of formulation. J Control Release 143: 13-22.

153. Gabizon AA (1994) Liposomal anthracyclines. Hematol Oncol Clin North Am 8:431-450.

154. Turk MJ, Waters DJ, Low PS (2004) Folate-conjugated liposomes preferentially target macrophages associated with ovarian carcinoma. Cancer Lett. 213: 165-172.

155. Gabizon A, Price DC, Huberty J, Bresalier RS, Papahadjopoulos D (1990) Effect of liposome composition and other factors on the targeting of liposomes to experimental tumors: biodsitribution and imaging studies. Cancer Res 50: 6371-6378.

156. Gabizon A, Shiota R, Papahadjopoulos D (1989) Pharmacokinetics and tissue distribution of doxorubicin encapsulated in stable liposomes with long circulation times. J Natl Cancer Inst 81:1484-1488.

157. Hwang KJ (1987) Liposome pharacokinetics. In: Ostro MJ (Ed.), Liposomes: From Biophysics to Therapeutics. Marcel Dekker, New York, USA 109-155.

158. Gregoriadis G (1988) Fate of injected liposomes: observations: observations on entrapped solute retention, vesicle clearance, and tissue distribution in vivo. In: Gregoriadis G (Ed.), Liposomes as Drug Carriers: Recent Trends and Progress. John Wiley and Sons, Chichester, England 3-18.

159. Huang SK, Lee KD, Hong K, Friend DS, Papahadjopoulos D (1992) Microscopic localization of sterically stabilized liposomes in colon carcinoma-bearing mice. Cancer Res 52: 5135-5143.

160. Huang SK, Martin FJ, Jay G, Vogel J, Papahadjopoulos D, et al. (1993) Extravasation and transcytosis of liposomes in Kaposi's sarcoma-like dermal lesions of transgenic mice bearing the HIVtat gene. Am J Pathol 267: 1275-1276.

161. Harrington KJ, Rowlinson-Busza G, Syrigos KN, Uster PS, Abra RM (2000). Biodistribution and pharmacokinetics of ^{111}In-DTPA-labelled pegylated liposomes in a human tumor xenograft model: implications for novel targeting strategies. British J of Cancer 83: 232-238.

162. Harrington KJ, Mohammadtaghi S, Uster PS, Glass D, Peters AM, et al (2001) Effective targeting of solid tumors in patients with locally advanced cancers by radiolabeled pegylated lyposomes. Clin Cancer Res 7: 243-54.

163. Dams ETM, Laverman P, Oyen WJG, Storm G, Scherphof GL, et al. (2000) Accelerated blood clearance and altered biodistribution of repeated injections of sterically stabilized liposomes. 292: 1071-1079.

164. Litzinger DC, Buiting AMJ, van Rooijen N, Huang L (1994) Effect of liposome size on the circulation time and intraorgan distribution of amphipathic poly(ethylene glycol)-containing liposomes. Biochim Biophys Acta 1190: 99-107.

165. Lui D, Mori A, Huang L (1992) Role of liposome size and RES blockade in controlling biodistribution and tumor uptake of GM1-containing liposomes. Biochim Biophys Acta 1104: 95-101.

166. Kong G, Braun RD, Dewhirst MW (2000) Hyperthermia enables tumor-specific nanoparticle delivery: effect of particle size. Cancer Res 60: 4440-4445.

167. Harrington KJ, Rowlinson-Busza G, Syrigos KN, Uster PS, Vile RG, et al. (2000) Pegylated liposomes have potential as vehicles for intratumoral and subcutaneous drug delivery. Clinical Cancer Res 6: 2528-2537.

168. Menaa F, Menaa B (2012) Development of mitotane lipid nanocarriers and enantiomers: two-in-one solution to efficiently treat adreno-cortical carcinoma. Cur Med Chem 19: 5854-5862.

169. Allolio B, Fassnacht M (2006) Clinical review: Adrenocortical carcinoma: Clinical update. J Clin Endocrinol Metab 91: 2027-2037.

170. Maluf DF, de Oliveira BH, Lalli E (2011) Therapy of adrenocortical cancer: present and future. Am J Cancer Res1: 222-232.

171. Berruti A, Terzolo M, Sperone P, Pia A, Casa SD, et al. (2005) Etoposide, doxorubicin and cisplatin plus mitotane in the treatment of advanced adrenocortical carcinoma: a large prospective phase II trial. Endocr Relat Cancer 12: 657-666.

172. Mehnert W, zur Mühlen A, Dingler A, Weyhers H, Müller RH (2007) Solid lipid nanoparticles (SLN)-ein neuartiger Wirkstoff-Carrier für Kosmetika und Pharmazeutika. II. Wirkstoffinkorporation. Freisetzung und Sterilisierbarkeit. Pharm Ind 59: 511-514.

173. Müller RH, Mäder K, Gohla S (2000) Solid lipid nanoparticles (SLN) for controlled drug delivery - a review of the state of the art. Eur J Pharm Biopharm 50: 161-177.

174. Mehnert W, Mäder K (2001) Solid lipid nanoparticles: production, characterization and applications. Adv Drug Deliv Rev 47: 165-196.

175. Pandey R, Sharma S, Khuller GK (2005) Oral solid lipid nanoparticle-based antitubercular chemotherapy. Tuberculosis (Edinb) 85: 415-420.

176. Couvreur P, Vauthier C (2006) Nanotechnology : Intelligent design to treat complex disease. Pharm Res 23: 1417-1450.

177. Yuan F, Dellian M, Fukumura D, Leunig M, Berk DA, et al. (1995) Vascular-permeability in a human tumor xenograft: Molecular-size dependence and cutoff size. Cancer Res 55: 3752-3756.

178. Torchilin VP (2005) Recent advances with liposomes as pharmaceutical carriers. Nat Rev Drug Discov 4: 145-160.

179. Hobbs SK, Monsky WL, Yuan F, Roberts WG, Griffith L, et al. (1998) Regulation of transport pathways in tumor vessels: Role of tumor type and microenvironment. Proc Natl Acad Sci USA 95: 4607-4612.

180. Harris JM, Martin NE, Modi M (2001) Pegylation: A novel process for modifying pharmacokinetics. Clin Pharmacokinet 40: 539-551.

181. Molineux G (2002) Pegylation: engineering improved pharmaceuticals for enhanced therapy. Cancer Treat Rev 28:13-16.

182. Djordjević A, Bogdanović G, Dobrić S (2006) Fullerenes in biomedicine. J BUON 11: 391-404.

183. Sitharaman B, Asokan S, Rusakova I, Wong MS, Wilson LJ (2004) Nanoscale aggregation properties of neuroprotective carboxyfullerene (C$_3$) in Aqueous Solution. Nano Letters 4: 1759-1762.

Author Affiliation

[1]Department of Bioengineering, University of Illinois, Chicago, USA